2019

Alterations in Stream Flow Associated with Gypsy Moth Outbreaks: A Remote Sensing Water Balance Approach

Sarah Smith-Tripp
ssmithtr@wellesley.edu

Alterations in Stream Flow Associated with Gypsy Moth Outbreaks: A Remote Sensing Water Balance Approach

Sarah Monroe Smith-Tripp

Submitted in Partial Fulfillment
of the
Prerequisite for Honors
in Geosciences
under the advisement of Jackie Hatala Matthes

April 2019

TABLE OF CONTENTS

TABLE OF FIGURES

ACKNOWLEDGEMENTS

My passion and capability for this work started years before the paper you read today. First and foremost, I must thank my advisor, Professor Jackie Hatala Matthes, for introducing me to the world of modeling and showing me quantitatively that everything is connected *and* that there is data available to prove it! I cannot thank you enough for supporting me when I came up with oddball ways to analyze data or when I sent drafts containing nothing but speculative section headings. Put simply, I would have been lost among millions of data points without your help.

I must secondly thank members of my committee Professor Dan Brabander and Professor Alden Griffith. Dan, the entirety of this research is based on mass balance, a concept that I learned from you as a young and inquisitive sophomore. Thank you for helping me internalize that it is the quality, not the quantity of research you do.

Alden, I don't think you or I realized that my fire project would ignite a passion for disturbance ecology that has carried into this thesis and beyond. So thank you for letting me grow and burn my "bromie homies." Thank you as well for the endless hours helping with statistics, R, GIS, and the weekly destress meetings critical to the production of the text before you. Similarly, I would like to thank EcoLab Research Assistant Sarah Russell for her patient help with R coding.

My research is entirely sourced from remote-sensing systems, so I thank the thousands of people required to operate USGS stream gages and data portal. I also thank Valerie Pasquerella of University of Massachusetts Amherst for generously allowing me to use her defoliation data product.

I cannot deny that my passion for water runs in the family. So I thank my mother, Susan Smith, for teaching me water is a privilege of our political, social and ecologic environment. To my other mother, Susan Tripp, thank you for always calling to check on me. And Marguerite, thank you for being willing to look over last-minute drafts.

I thank Wellesley geosciences for being my home away from home these past four years. The positive influence geosciences has had on my life and the way I approach big data problems cannot be stated in words. To the other thesising geoscience seniors, thank you for the comradery we shared and will continue to share. To my roommate and best friend Jenn Harris, thank you for being a friend in the dark and light portions of this thesis and year. To Kimberly Chia Yan Min – you are an inspiration for

research, dedication, and unabashed kindness. Thank you for all of the observatory, module, and random coffee shop “thesis camps” throughout this year. In the name of my self-care, I thank my running buddy Sam Muller for helping me get out of bed, on the track, and onto my thesis.

Finally, I thank the larger Wellesley community, including committee member Professor Thomas Hodge, for balancing my education with coursework and opportunities all over the world. My experiences at Wellesley and away taught me how humans are connected to their environment and how this connection is perturbed by disturbance events. Natural processes affect and connect us, but yet in so many ways, act independently of us. A quandary perhaps best described, although unanswered, by nature writer Ivan Turgenev:

> “Without question, in her entirety [Nature] constitutes one great, well-proportioned whole — every point within her is united with every other point — but at the same time her aspiration is that precisely each point, each separate unit within her, exist exclusively for itself, consider itself the center of the universe, turn to its own advantage everything around it, negate the independence of those surroundings and take possession of them as its own property.”
>
> – Turgenev, second review of Aksakov's *Notes of an Orenburg-Province Hunter*

ABSTRACT

Background/Question/Methods

The quality and quantity of water resources in the Northeastern United States are reliant upon forested watersheds. In this area, water resources are sourced from shallow aquifers and groundwater storage, which are both closely tied to surface ecosystems. Rates of evapotranspiration are specifically determined by environmental conditions and plant traits of a particular ecosystem. The interconnected nature of water resources to surfaces processes in southern New England makes understanding interactions between ecosystem disturbance and hydrology particularly important. The gypsy moth is a forest insect whose larvae consume leaves of broad-leaved trees. Outbreaks of this insect cause regional decrease in leaf area, which is related to rates of evapotranspiration. This study directly compares seasonal stream discharge during the 2015-2017 gypsy moth outbreak and defoliation to periods of non-defoliation. I hypothesized that decreased evapotranspiration associated with reduced leaf area from would increase flow intensity and discharge produced in proportion to defoliation. To test these hypotheses, this research integrated remotely sensed imagery of gypsy moth defoliation severity with data from USGS stream gages and Daymet precipitation data to understand and quantify the impact of the 2015-2018 gypsy moth outbreak on water resources in southern New England.

Results/Conclusions

I found the intensity of defoliation varied greatly annually and over the southern New England hydrologic landscape. Additionally, I found that there was a strong association between increased defoliation and an increased proportion of precipitation exiting a watershed as discharge. By definition of the water balance equation, this increased discharge supports changes in evapotranspiration associated with defoliation are measurable at downstream locations. The magnitude of discharge increase was most apparent at normal and low flow conditions. Discharge increase associated with defoliation is a consistent increase in the amount of water measured at the stream gage. In the context of broader literature, the intense defoliation of 2016-2018 raises important questions for the stability of the forest community and spread of gypsy moth. Increased discharge rates similarly alter the sedimentation and nutrient loading in a watershed. This study recommends future work to focus on how discharge, sedimentation, and nutrient flux are altered by a disturbance, particularly in areas newly affected by gypsy moth outbreaks.

INTRODUCTION

1.1 INFLUENCE OF FOREST VEGETATION ON WATER YIELD AND QUALITY

Forested watersheds drive the quality and quantity of water resources in the Northeastern United States. In southern New England specifically, 10.2 million people rely on water resources from forested ecosystems (Barnes *et al.*, 2009). The southern New England area is one of the most densely populated and urbanized locations in the Northeastern United States (Barnes *et al.*, 2009). In this area, water is sourced from shallow aquifers and ground water storage, which are both closely tied to surface ecosystems. New England water storage and transport is restricted mainly to upper permeable soils, which can be rapidly depleted through evapotranspiration by trees in drought conditions (Johnson *et al.*, 2016; Easton *et al.*, 2007). The proximity of water to the surface also means that nutrient composition is affected by above-ground forest processes (Moore *et al.*, 1978; Easton *et al.*, 2007; Clark *et al.*, 2014). Thus, water resources in this heavily populated area are critically coupled with forest hydrology and ecosystems.

Water quality is reliant on the overall health of the watershed (Barnes *et al.*, 2009). Forests provide free ecosystem services such as filtration and pollutant removal that are otherwise are labor and cost intensive services provided by water treatment plants. Additionally, forests supply long term storage to aquifers, absorbing groundwater that otherwise is lost through pavement (impervious land) associated with development. It is generally considered more cost-efficient and effective to protect a forest than to treat the water (Barnes *et al.*, 2009). Increasing amounts of impervious land (caused by paving associated with development of roads, parking lots, and building structures) means that ground-water infiltration is increasingly limited to forested areas and storm runoff drains (Barnes *et al.*, 2009; Easton *et al.*, 2007). In the rapidly developing southern New England area, water resource management should carefully consider the influence of remaining forest vegetation on water yield and quality.

Figure 1: Importance of watersheds for drinking water. Watersheds ranked according to their Ability to Produce Clean water (APCW) including the amount of forest, and the number of consumers served. *Figure Sourced: Barnes et al. (2009*)

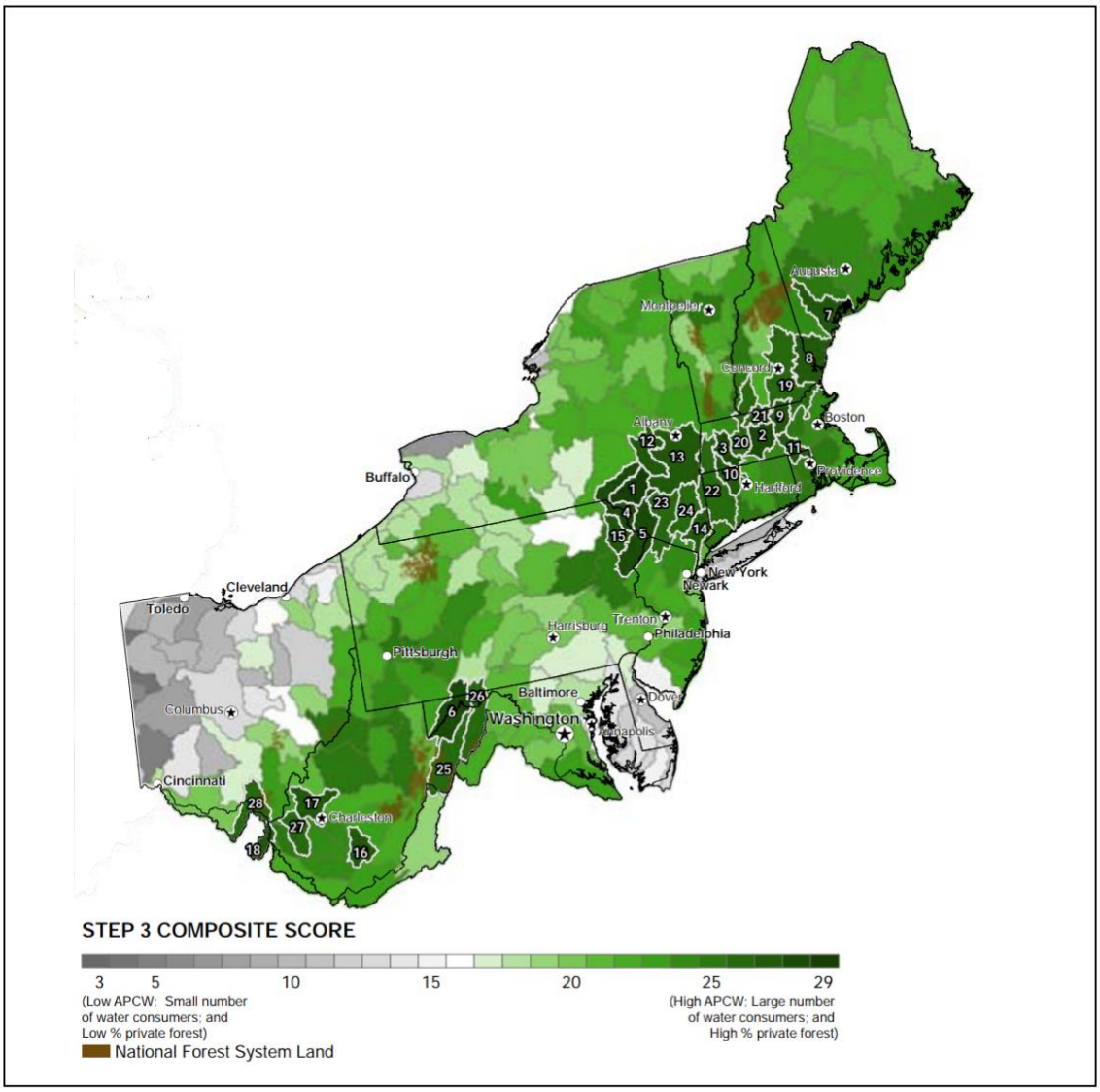

During the growing season in a typical forest ecosystem evapotranspiration through trees can dominate water flux out of the system (Dingman, 2015). Temperature fluctuation and tree growth rates can dramatically affect the rate of evapotranspiration, and thus stream discharge (Kendall and McDonnell, 2012; Rustad *et al.*, 2012). Meta-studies of watershed vegetation change show that decreased vegetative cover causes quasi-linear increases in water yield over short time scales (Figure 2; Brown et al, 2005; Bosch and Hewlett, 1982).

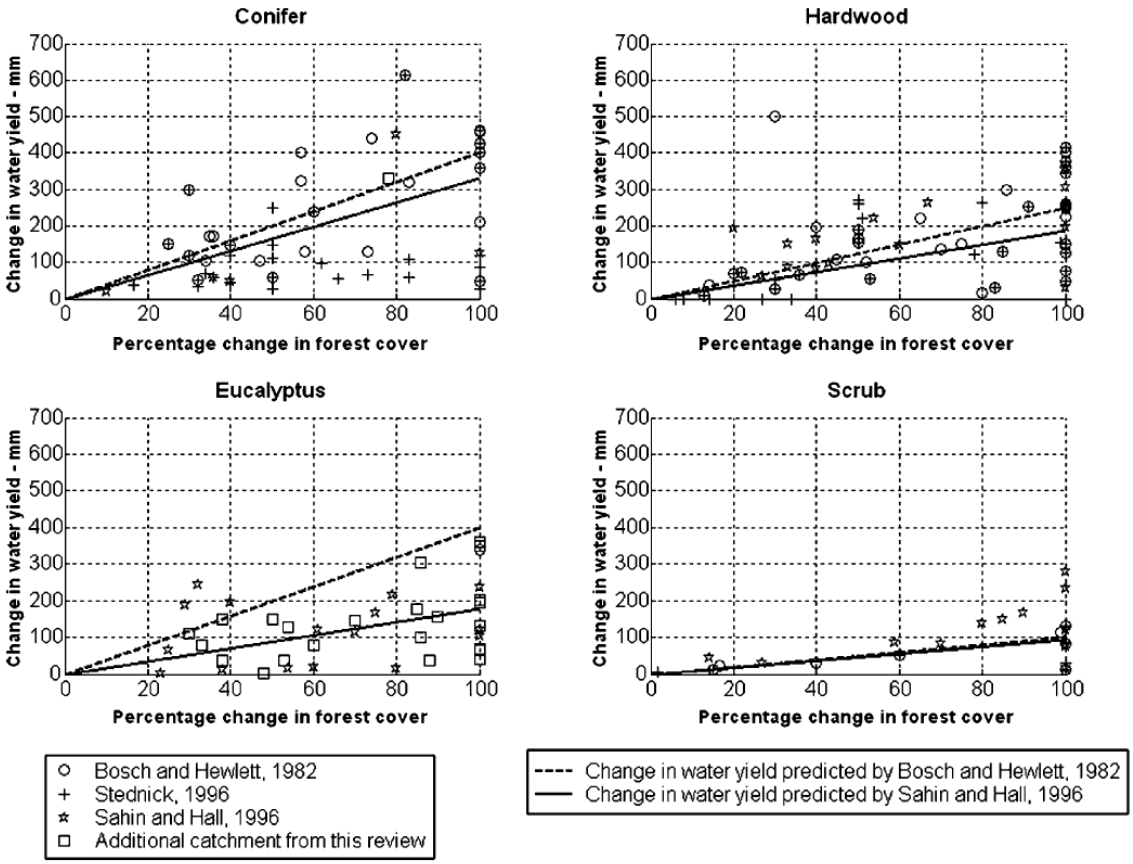

Figure 2 Data from review of global watershed studies with decreased forest cover. *Figure source: Brown et al., 2005.*

These studies provide strong evidence that the flux of water in a watershed (assuming a constant long-term storage pool) can be described as follows:

$$Discharge \propto precipitation - evapotranspiration$$ (Chapin III *et al.*, 2011)

Evapotranspiration (*ET*) is controlled by water availability, plant traits (stomatal resistance, leaf area index, plant height, and plant morphology) and meteorological factors (temperature, humidity, photon flux density) (Kendall and McDonnell, 2012). Thus, rates of evapotranspiration are specifically determined by environmental conditions and plant traits within a particular ecosystem. As a result, while decreased vegetation cover causes increases in annual water yield, the effect size varies significantly by forest and climate type (Brown *et al.*, 2005). In the Northeast specifically, a summary of experiments in the Hubbard Brook Experimental Forest in New Hampshire found that deforestation of a watershed caused up to a

67% increase in growing season water yield (Hornbeck *et al.*, 1997). From this finding, they concluded that effective water management schemes should incorporate portions of deforested land to decrease the likelihood of water shortages (Hornbeck *et al.*, 1997). However, along with the positive aspect of increased water yield, the potential negative effects of increased run-off on soil erosion and decreased water quality in terms of turbidity must also be considered.

1.2 Risk of Disturbance with Altered Climate and Shifted Plant Communities

The water balance and forest ecosystems of the mixed hardwood and oak-pine forests that dominant southern New England are impacted by a changing climate and anthropogenic activity. In the past 100 years, the Northeast area has become warmer and wetter (9% greater precipitation) and has had an 8% increase in the number of extreme precipitation events (Rustad *et al.*, 2012). The majority of this shift occurs in the spring and fall. In addition to increased precipitation, the frequency of (mostly of short-term) droughts has also increased (Rustad *et al.*, 2012; Huntington *et al.*, 2009; Hayhoe *et al.*, 2007). With warming during spring and fall, the length of the growing season is increasing, which is of particular importance for dominantly deciduous forests in the Northeast (Hayhoe *et al.*, 2007).

Increased frequency of droughts in Northeastern forests stresses plants, increasing risk of mortality by a drought or other disturbance. Disturbances are events that dramatically alter ecosystem functions (photosynthesis, transpiration, carbon-storage, species composition) and are short on ecological timescales. They include events like insect infestations, wind storms, droughts, and wildfires. Small to moderate disturbances like short term insect infestations or low-temperature fires often decrease plant-plant competition and can have a positive effect on diversity, species richness, and habitat quality. However, services like fresh water, carbon storage, and timber harvest, which rely on consistent forest function, can be detrimentally affected by disturbances (Thom & Seidl, 2016). In the Northeast, where groundwater storage is limited and relatively surficial, Barnes *et al.*(2009) argue that successful watershed protection is "deliberately patterned across the landscape to be resistant and resilient after natural disturbances."

Most ecosystems, including Northeastern forests, are adapted to typical disturbance regimes and are thus resilient in the face of ordinary disturbances; however novel disturbances and multiple stressors are particularly disruptive for all ecosystem types (Seidl *et al*., 2017). Increased climate variability associated with climate change increases disturbance intensity and duration (Thom & Seidl, 2017). Longer, chronic and more intense disturbances are likely to push ecosystems to "thresholds" beyond which major ecological transformations ensue. Understanding when chronic or high-intensity disturbance causes major ecosystem alteration (i.e. wide-spread mortality) is important for informing forest mitigation strategies that maintain ecosystem services (Millar & Stephenson). Additionally, many disturbances increase the likelihood and scale of additive or synergistic disturbance impacts. For example, an ecosystem experiencing drought would be more likely to also experience an insect outbreak (Seidl *et al.*, 2017). Northeastern forests are well adapted to low-level periodic disturbances (fire and insects), but the current large-scale and multiplicative forest disturbances are at intensities that the Northeast has not experienced since European deforestation (Nowacki and Abrams, 2015).

1.3 Impact of Forest Insect and Pathogen Disturbances on Hydrology

Studies of the impacts of disturbance on stream hydrology are extensive but are concentrated on the impacts of logging and fire (Brown *et al.*, 2005). Of these studies, most are focused on somewhat planned disturbances like logging and fire, where follow-up stream sampling schemes are easy. Additionally, these hydrologic investigations are often limited because changes in stream hydrology are typically negligible when the change in vegetation of the watershed is less than 20% (Bosch and Hewlett 1982; Brown *et al.*, 2005). While the impact of planned disturbance events is well studied, the impact of unplanned disturbances (particularly forest insects) is less well known.

Forest insects affect an area 45 times greater than wildfire and cost $1.5 billion dollars in damage each year (Hicke *et al.*, 2012). Insects are difficult to study because outbreak extent and timing are unpredictable. Published work on the hydrological changes associated with insect disturbances is concentrated on bark beetles in the Western U.S. (Weed *et al.*, 2013). A study of pine beetles, which cause rapid tree mortality by impeding the flow of water through

tree xylem, found that water discharge from impacted watersheds was 30 (+/- 15) % greater than unaffected neighboring watersheds (Bearup *et al.*, 2014). In a study on the hemlock woolly adelgid at the Harvard Forest in central Massachusetts, Kim *et al.* (2017) found that there was a 15.6% annual increase in stream discharge as well as a 24-37% decrease in evapotranspiration during hemlock woolly adelgid infestations. However, the hemlock wooly adelig study has limited application to deciduous Oak and Maple forests of southern New England, which differ from coniferous hemlocks in transpiration rates in a short-term and seasonal scale. Both of these studies support there can be a large-scale change in water yield due to forest insect or pathogen disturbance.

The increased exposure of Northeastern forests to disturbances and the emergence of less drought-tolerant landscapes underscores the need for an integrated approach to studying hydrology, insect outbreaks, and resulting dynamics in forest ecosystems. Since hydrological flows are the emergent outcome of complex drivers (vegetation, climate, and disturbance extent), understanding *ET* at a watershed scale could be critical for local water management.

1.4 2016-2018 Case Study: The Gypsy Moth

The gypsy moth was accidentally introduced to the Northeast in the late 1860s (Liebhold *et al.*, 1992). Since their introduction, gypsy moth caterpillars have acted as a prominent defoliator (leaf-eater) of Eastern U.S. forests. They are generalist defoliators, with a preference for oak species, but will consume leaves of any hardwood species in outbreak years. Defoliation of trees is most intense in the early spring (May and June), when larvae emerge and consume young buds and tree leaves (Doane and McManus, 1981; Liebhold *et al.*, 1992).

According to tree species and current gypsy moth distribution, about 62% of southern New England forests are susceptible to gypsy moth outbreaks (Liebhold *et al.*, 1997) The spread of gypsy moth has been well investigated and modeled (Doane and McManus, 1981). When first released, gypsy moths spread rapidly across the Northeast, but population growth slowed when pest control strategies (including DDT) were utilized (1950s to 1970s). Following a decrease in eradication efforts and insecticide use in the 1970s, the range of gypsy moths

quickly expanded (1970s to 1990s) (Liebhold *et al.*, 1992). The current range of the gypsy moth includes all of the Northeast, Mid-Atlantic, and Michigan (Liebhold *et al.*, 1992).

Since 2015, a gypsy moth (*Lymantria dispar*) outbreak has created multiple large-scale defoliation disturbances in the southern New England region. The suspected cause of their emergence is related to a series of dry springs from 2014-2016 that supported outbreak conditions continuing into 2018 (Pasquerella *et al.*, 2018). Rhode Island NOAA Climate Data (aggregated from numerous weather stations statewide) shows a long period of dry growing seasons starting in 2014 (Figure 2; NOAA, accessed Apr. 17, 2019).

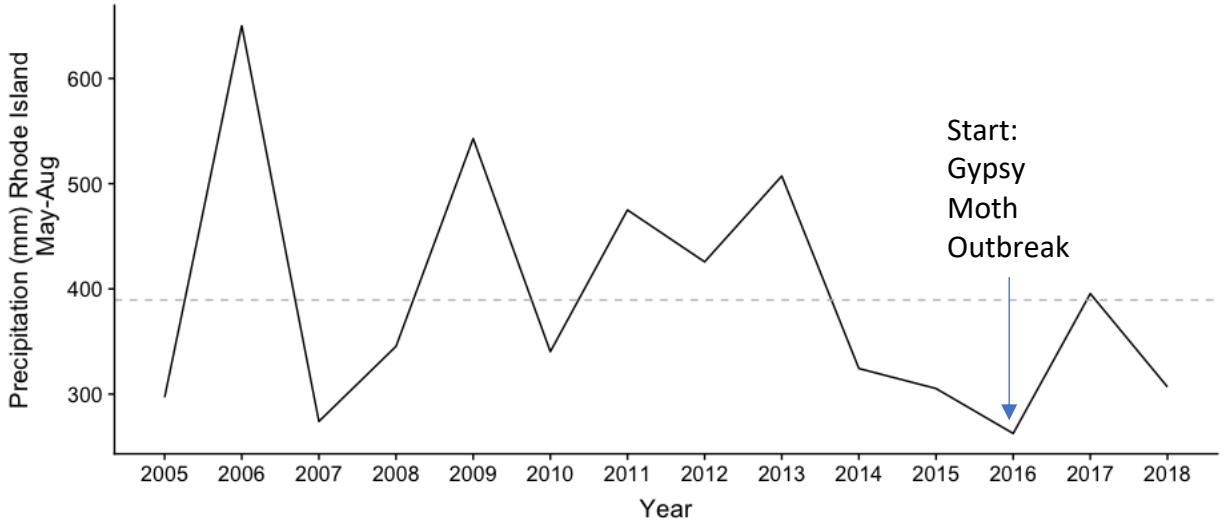

Figure 3: NOAA precipitation in mm for the state of Rhode Island from 2015 -2018. Precipitation data aggregated of all NOAA monitoring locations. The grey line shows the 10-year average rainfall from 2005-2014. (*Data sourced:* NOAA, accessed Apr. 17th, 2019)

Gypsy moth outbreaks are favored by drought conditions. Past research has shown that prior year's rainfall is an effective predictor of outbreak conditions (Miller *et al.*, 1989). Drought conditions are known to decrease the effectiveness of *Entomophaga maimaiga* a fungal pathogen. Without rain, fungal spores of *Entomophaga maimaiga* dry out decreasing germination and the effectiveness of the pathogen as a biocontrol agent (Elkinton and Boettner, 2016; Hajek *et al.*, 1996). Another major biologic control, *Lymantria disparnucleovirus* is highly effective at killing gypsy moths, but only when populations are in outbreak conditions

(Elkington and Boettner, 2016). The cause of the 2016 outbreak, which was the worst outbreak since 1981, is attributed to the intense drought beginning in May of 2014 that caused a decrease in the effectiveness of *Entomophaga maimaiga* (Elkinton and Boettner, 2016; Figure 3).

Once established in a location, gypsy moths follow a period of cyclic outbreaks. The periodicity of these outbreaks is generally dependent on geographic location, forest-type, and climate factors (Johnson *et al.*, 2006). In the oak-pine forests of southern New England, gypsy moth outbreaks have a long periodicity, occurring on an 8- to 10-year scale, with smaller outbreaks occurring every 4 to 5 years (Johnson et al, 2006). However, conditions influencing the intensity and duration of an outbreak in an infested area are less understood than periodic outbreak cyclicity (Johnson *et al.*, 2006). Gypsy moth infestations differ from other forest insects in the northeast, including the previously discussed hemlock wooly adelig, because gypsy moths prefer deciduous oak trees and infestations are intense and relatively stochastic. Hemlocks wooly adelgid infestations affect coniferous trees and have a long duration and moderate intensity (Kim *et al.*, 1981).

Areas of periodic outbreaks often have multiple years of successive defoliation, particularly in oak forests. About 14% of areas defoliated between 1974 and 2010 experienced successive years of defoliation, 85% of these areas were oak and hickory forest types (Morin and Liebhold, 2016). In the Northeast, gypsy moth defoliation peaked in the 1980s (Morin and Liebhold, 2016; Elkinton et. al., 1990). Since the 1980s, *Lymantria dispar nucleopolyhedrovirus*, an introduced virus, in combination with *Entomophaga maimaiga*, an introduced fungal pathogen, have acted as a biocontrol keeping outbreak levels low (Hoover *et al.*, 2011; Hajek *et al.*, 1996). The recent 2016 outbreak, which is the first major outbreak in southern New England since 1980, has impacted Rhode Island most dramatically (Pasquarella *et al.*, 2017; Elkinton and Boettner, 2016).

1.5 Impact of Gypsy Moth on Forest Hydrology

Defoliation by gypsy moths and other defoliators can have important consequences for tree stress and stand mortality. Dietze and Matthes (2014) modeled stressors over multiple

years and found that defoliation decreased growth potential of trees, but trees mostly recovered after one year of defoliation. Over 4 years of successive defoliation, the forest stand had decreased in net ecosystem carbon exchange (a measure of stand growth; Dietze and Matthes, 2014). This suggests that successive years of defoliation can change overall stand productivity in and alter ecosystem dynamics. Dietze and Matthes (2014) also found defoliating insects increased soil moisture dramatically in the first year of invasion, particularly when compared to other insect functional types. It is thus important to investigate if large defoliation events, like that of 2016, have implications on stream hydrology (or the ecosystem water balance) over the long and short term.

Studies of changes to hydrology that are associated with defoliation of gypsy moths are extremely limited, and the few that exist are concentrated in the New Jersey pine barrens (Clark *et al.*, 2012). In the 1970s, a study occurred using a series of gypsy moth plots with successive levels of defoliation (Doane and McManus, 1981). Preliminary work on the effect of gypsy moth defoliation found that a 75% vegetation coverage reduction resulted in a 1365m^3 increase in stream discharge, but, details regarding the research study's experimental design are not available, and thus this number cannot be contextualized (Doane and McManus,1981). More recent studies found that gypsy moth defoliation was associated with a decrease in evapotranspiration in oak forests and pine forests. Using analyses of decreases in evapotranspiration, LAI, and forest canopy cover, Clark *et al.* (2012) estimate that groundwater recharge rate during defoliation is 7.3% higher than pre-defoliation periods. These research methods did not include a watershed water yield or flow-regime analyses. To support their speculations of increased ground-water recharge associated with defoliation, focused research on the ecosystem water balance is required.

1.6 Objectives of Current Research

Considering the importance of stream hydrology to freshwater availability in southern New England and the unique responses of watersheds to disturbance events, better knowledge of the 2015-2018 gypsy moth outbreak on forest hydrology is required. This study directly compares stream hydrology to gypsy moth defoliation in an oak-dominated forest of southern

New England. Importantly, the study considers how multiple years of defoliation, or extreme defoliation, can lead to fundamental changes in the ecosystem water balance.

The objectives of this study are as follows:

1. To assess whether gypsy moth defoliation events are associated with alterations in flow characteristics
2. To quantify how defoliation intensity scales to short-term changes in discharge volume relative to precipitation during the growing season

As defoliators, gypsy moth disturbances lead to loss of leaf biomass and surface area. Leaves are the conduits for evapotranspiration in trees. Due to this evapotranspiration relationship, I hypothesize that gypsy moth invasions will decrease evapotranspiration and interception by the tree canopy. This decrease in evapotranspiration will theorectically increase runoff and groundwater flow. A schematic diagram flow into the watershed (dominated by precipitation) and flows out of a watershed (dominated by groundwater, runoff, and evapotranspiration) is shown in **Figure 4**. As a simple model, I hypothesize that discharge can be scaled by some function of X which includes some non-zero rate α and where X is metric for defoliation. I hypothesize that greater rates of defoliation will see a greater deviation from the baseline of stream discharge. To test these hypotheses, this research integrates remotely-sensed imagery of gypsy moth defoliation severity with data from USGS stream gages and Daymet precipitation data to understand and quantify the impact of the 2015-2018 gypsy moth outbreak on water resources in Rhode Island.

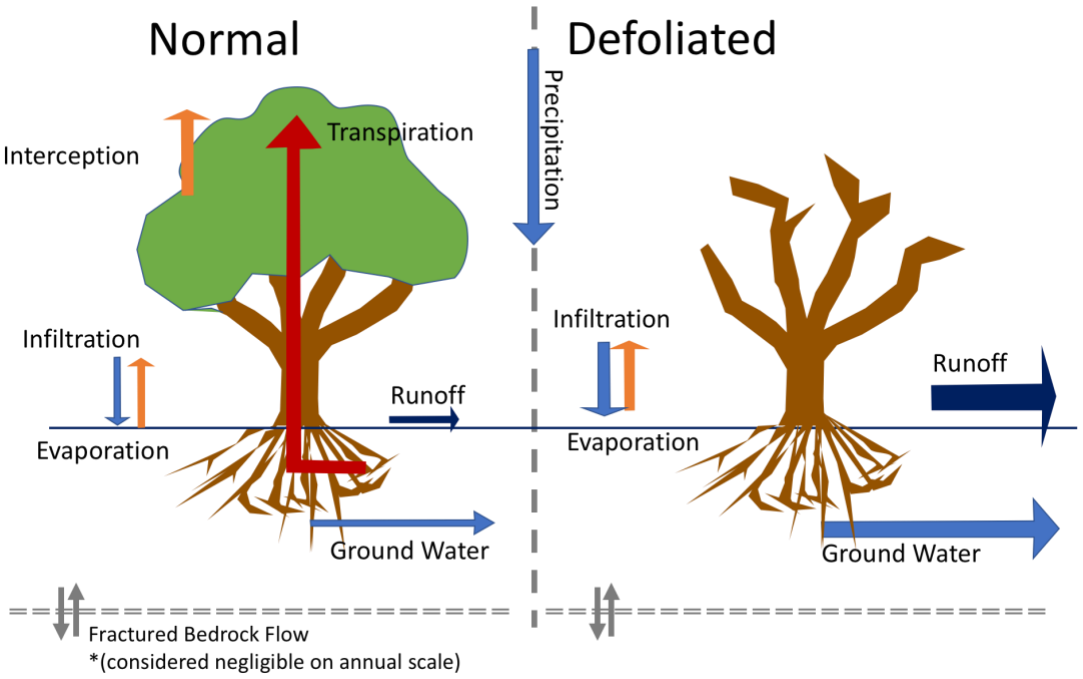

Figure 4: Hypothetical Alterations in Evapotranspiration, Runoff, and Groundwater infiltration given Gypsy Moth Defoliation. Normal, non-defoliated conditions are shown on the left. Defoliated conditions shown on the right. Arrow size shows relative changes and is not to scale.

2. METHODS

2.1 REGIONAL DEFOLIATION INTENSITY AND EXTENT

A series of dry Northeastern springs from 2014-2016 is thought to have decreased the effectiveness of fungal pathogen *Entomophaga maimaiga* that regulated populations of gypsy moth starting in the 1980s (Elkington and Boettner, 2016). As a result, southern New England saw the most widespread and intense series of defoliation events in these hardwood forests since the virus's introduction. There is an increase in the threat of large-scale gypsy moth defoliations like the defoliation of 2015 – 2018 because of a high likelihood of gypsy moth range expansion and population proliferation during drought conditions (Huntington *et al.*, 2009; Liebhold *et al.*, 1994).

My thesis study used the annual mean defoliation data for 2015, 2016, and 2017 provided by Pasquerella *et al.* (2017) to assess changes in watershed foliation at a growing season scale. To quantify the extent and intensity of the 2015-2017 defoliation, Pasqueralla *et al.* (2018) used Landsat satellite imagery to produce a regional defoliation data product. Their method calculated defoliation using a continuous change and detection classification algorithm based on a model of tasseled cap greenness. In this data product, defoliation in 2015-2017 was compared to model produced expected greenness from the prior decade (2005-2015). Defoliation was quantified as the residual (i.e. the difference) between tasseled cap greenness in each Landsat image in the growing season of 2015-2017 to the expected mean greenness on that date, where negative values indicate defoliation (lower greenness values). Values used in the present study are standardized amongst images by dividing raw differences by the root mean square error to produce the units used in this study. These units describe the difference in measured Tasseled Cap Greenness relative to unexplained variability. This approach allowed for near-real-time assessment of defoliation, even when pixels were obscured by cloud cover. Individual pixels for each Landsat image taken at approximately 2-week intervals were combined during the growing season to create an annual mean defoliation index for each Landsat pixel during the defoliation period (see an example of annual defoliation raster in Figure 5; Pasqueralla *et al,* 2018).

I used the defoliation raster data product to evaluate defoliation intensity within each watershed of the study area. Watersheds were delimited by the USGS watershed boundary dataset (WBD; USGS *et al.*, 2018). The WBD for hydrologic unit 01 (the northeast) includes both watershed and sub-watershed data at a 1:25,000 scale. Hydrologic unit codes (HUC) include watershed name, watershed type, and list major alterations in the watershed. Hydrologic Unit Code 01 (HUC01) is the Northeastern WBD and includes 8 progressive levels of watershed delineation, from 2-digit to 12-digit (USGS *et al.*, 2018). This study follows standard practice using 10-digit or "watershed" level unit code for watershed analysis. (USGS *et al.*, 2018). I created a subset of HUC 01 that included Massachusetts, Connecticut, and Rhode Island. I excluded watersheds that overlapped with neighboring states (New York, Vermont, and New Hampshire). Massachusetts and Rhode Island include both standard hydrologic units (where there is one point of discharge in the watershed) and frontal discharge unit types (where there are multiple drainage locations e.g. into a bay). Using vector shapefiles of the 10-digit watersheds and the defoliation value of each grid cell in the watershed, I used QGIS 3.14 zonal statistics to calculate the mean defoliation for each year (USGS *et al.*, 2018).

2.2 USGS STREAM GAGE DATA

To quantify potential changes in stream flow, I used data from 89 USGS stream gages that covered the southern New England region and downloaded stream discharge data during the 2015-2017 defoliation time period from the national hydrology dataset (NHD; USGS, 2004; Fig 1). Stream gages were selected based on categories available from the GAGES – II dataset (Falcone, 2011). Stream gage selection criteria were (1) the stream gage must have more than 18 years of data from 1990 to 2009 and (2) the stream gage was active in 2009. Stream gages were located mostly in standard watershed types, with one stream gage located in a frontal discharge watershed. This analysis included 14 reference stream gages based on definitions provided by Falcone (2011). Reference stream gages are in locations where there is minimal human impact to hydrology and the flow is considered to be near natural. These reference stream gages also include at least 20 years of historical data in their record. In this study, analyses were separated into changes within reference gages only, and all stream gage types. I

assume changes at reference gages are better constrained to changes in the vegetation rather than associated with anthropogenic development. To quantify total seasonal discharge, I downloaded average daily discharge data in cubic feet per second from May 1, 1998 to present for stream gages using the waterData R package using station ID numbers of the stream gages provided in the NHD (Ryberg and Vecchia, 2012). The 20-year (1998-2018) time period was used because it is standard practice to use 20 years of discharge to characterize streamflow regimes. After downloading, I created a subset of discharge data that included values specific to the growing season (May to August).

I aggregated total seasonal discharge for all reference and non-reference stream gages for the 1998-2018 time period. I used the 2005-2014 time period as a baseline "pre-defoliation" dataset to compare against the 2015-2017 stream discharge during defoliation years. A decadal mean was selected as it is a common time frame used to assess climate norms like precipitation I also examined individual stream gages for substantial change in stream discharge characteristics from 1995-2015 baseline period by visually assessing trends in maximum daily discharge, mean daily discharge, 7-day minimum discharge, and the standard deviation of discharge using the EGRET water analysis package (Hirsch and Cicco, 2014).

To assess differences in flow characteristics between years with defoliation and baseline, I produced flow duration curves for each reference stream gage using data downloaded through the waterData R package and using the flow duration curve equation from the EGRET R package (Ryberg and Vecchia, 2012; Hirsch and Cicco, 2014). Flow duration curves characterize the likelihood of discharge events of different magnitudes within a stream by visualizing the statistical frequency of high-flow and low flow periods over a season or year (Hirsch and Cicco, 2014). In these curves, flow values that occur less than 75% of the time are considered "high-flows" or flood events. Values that occur between 75% and 25% of the time are representative of normal stream flow (McMahon *et al.*, 2003). Based on work in deforested watersheds, I expected that high time-fractions would have the greatest deviance from baseline, and that flow during floods or high flow events would increase (Hornbeck *et al.*, 1997) A model of this relationship and a simple schematic of a flow duration curve is shown in **Figure**

5. The relationship shown in **figure 5** is based on the hypothesis that groundwater and runoff flow increase with defoliation. I based the relationship shown in **figure 5** on a paired catchment study in deforested watersheds which supported increased discharge associated with deforestation (Hornbeck et al., 1997).

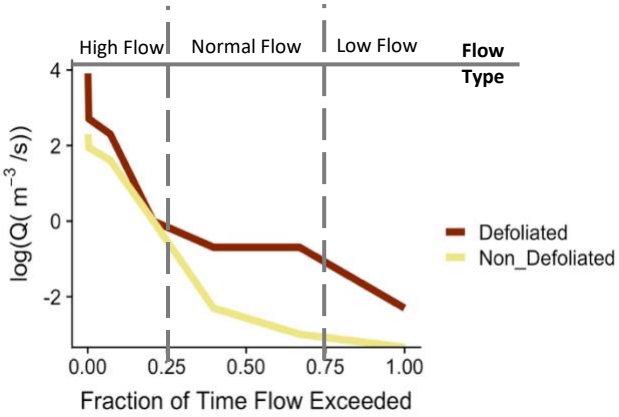

Figure 5: Hypothetical Relationships of a Flow Duration Curve In a Defoliated and Non-Defoliated Watershed. Fraction of time (X) that flow (Q; Y) is exceeded. Brown line represents hypothetical relationship in a defoliated stream, tan represents a non-defoliated stream. Approximate relationships based on paired catchment study of a deforested watershed in Hornbeck *et al.* (1997).

I produced flow duration curves for each individual reference stream gage using daily average discharge values downloaded in cubic feet per second and converted to m^3/s . I used the flow duration curves to assess whether defoliation intensity shifted the frequency of large magnitude events and other normal flow discharge values. A 20-year time frame (a typical length for a hydrologic study) was used to create a baseline curve of individual flow regimes for each stream. Flow duration curves for 2015, 2016, and 2017, were compared among each other and in comparison to the baseline curve.

2.3 Precipitation Data

To achieve high specificity in precipitation data I used Daymet produced precipitation values. Daymet is a model of daily meteorological parameters produced using interpretation and extrapolation of meteorological observations to produce a global one-kilometer by one-kilometer grid for metrological parameters (Thornton *et al.*, 2018). The Daymet data product is available at a one kilometer spatial resolution and daily observation from 1980 to the present day. I used the spatial coordinates for each stream gage to download the associated pixel of Daymet daily total precipitation (mm) from 1995-2017 for May through August using the

Daymetr R package (Thornton *et.al.,* 2018). Stream gage data point locations were converted from points from North American Datum 83 to World Geodetic System 84 to ensure that the location was specific to the gage location itself. Precipitation data is in millimeters per meter squared (mm/m^2)

I aggregated daily precipitation data from the Daymet data product (Thornton, *et.al.* 2018) to quantify the total growing season precipitation for the upstream area of each USGS stream gage station used in this study. To analyzed precipitation by year, I first quantified the intensity of precipitation using a density curve. The volume of the density curve was normalized to the total sum of precipitation in all stream gages. This allowed me to assess if individual years had a higher proportion of large precipitation events. Second, I compared the sum of growing season precipitation values measured at each stream gage location to assess how total precipitation varied by year in the southern New England stream gages.

2.4 WATERSHED MASS BALANCE

I used a mass-balance ratio approach to assess change in water mass balance at each stream gage. The watershed mass balance approach is based on the following discharge equation for a stream.

$$Q_{discharge} = Q_{precipitation} - Q_{evapotranspiration} - Q_{groundwater\ loss} - /+ \underline{\Delta}_{storage}$$

This study assumed that change in the storage is minimal at the temporal scale of this study (years). Additionally, this study assumed that the rate of groundwater loss is relatively constant or minimal in the overall flux of stream discharge. Following these assumptions, the revised stream discharge can be simplified as:

$$\underline{\Delta}\ Q_{discharge} = \underline{\Delta}\ (Q_{precip} - Q_{evapotranspiration} - Q_{interception})$$

I used this framework to assess whether changes in evapotranspiration and interception associated with gypsy moth defoliation altered the ratio between discharge and precipitation during the growing season (May through August). This ratio is henceforth referred to as discharge:precipitation. I scaled the Daymet precipitation data from a single point to the entire

watershed above each stream gage by multiplying by precipitation with the upstream watershed area included in the metadata of each stream gage. The following equation was used to convert from Daymet precipitation measurements ($\frac{mm}{day}$) to volume of precipitation of the drainage area of each stream gage during the growing season.

$$Volume\ Precipitation\left(\frac{m^3}{year}\right) = \sum_{year} \frac{mm}{day} * \frac{1\ m}{1000\ mm} *\ m^2_{drainage\ area}\ = \frac{m^3}{year}$$

I converted daily mean discharge data from each stream gage to a total value for each growing season. This transformation assumed constant flow over daily periods because it used the mean discharge (cfs) over the day. Data from stream gages were transformed according to the following equation:

$$Discharge\ \left(\frac{m^3}{year}\right) = \sum_{year} \frac{ft^3}{s} * \frac{60s}{1min} * \frac{60min}{1hr} * \frac{24hrs}{1\ day} * \frac{0.0283168m^3}{ft^3}$$

Using the total growing season precipitation and stream discharge, I calculated the annual discharge:precipitation for each stream gage in each year:

$$\frac{Discharge\ \left(\frac{m^3}{year}\right)}{Volume\ Precipitation\left(\frac{m^3}{year}\right)}$$

To better compare patterns across all watersheds, I avoided site-specific differences in the typical discharge:precipitation by calculating the difference between the 2015-2017 discharge:precipitation and the 2005-2014 decadal mean discharge:precipitation of each stream gage. Additionally, the differences between current and year prior mean discharge-to-precipitation ratio was ranked for all stream gages. Stream gages that appeared in the top twenty difference values more than once were removed from analyses. Ideally, this limited the number of watersheds that had large changes in flow dynamics not associated with defoliation events. From the decadal mean discharge:precipitation, I calculated residual discharge:precipitation as the difference between the specific year discharge:precipitation and the decadal mean.

For years during defoliation outbreak, I compared residual discharge:precipitation values to the mean residual defoliation in each watershed. Defoliation values for 2015, 2016, and 2017 were calculated from the zonal statistics over each pixel of the watershed area. Mean defoliation values were spatially joined to specific stream gages based on their respective watershed locations.

2.6 Statistical analysis.

For statistical analysis of the interaction of mean defoliation and discharge:precipitation, all analyses were run on all stream gages and reference gages that fit prior requirements (19 years of good data prior to 2009 and active in 2009). Prior to testing relationships between discharge:precipitation and defoliation, I tested the relationship between defoliation and drainage area of the stream gage. Drainage area was used to calculate the discharge:precipitation. This analysis tested for correlation amongst precursors to the final discharge:precipitation. An ANOVA statistical test was used to test for an interaction between mean defoliation and stream gage drainage area. A relationship between defoliation and drainage area was not found (Supplemental Information p = 0.30), which allowed testing of the association between discharge:precipitation and defoliation.

An ANOVA test was used to assess mean defoliation accounts for variation in discharge:precipitation. This study included year as an interaction factor in this analysis so that each relationship was analyzed as by individual year as well as the overall interaction. The output of the ANOVA details the response of discharge:precipitation, year, and the interaction of the two variables. The ANOVA was run on a linear model of the following equation in base R:

$$discharge{:}\,precipitation = mean\ watershed\ defolation * year$$

ANOVA results were used to test for the variance in the dependent variable (discharge:precipitation and year) associated with the variation in the given dependent variable (mean defoliation).

3. RESULTS

3.1 REGIONAL DEFOLIATION EXTENT AND INTENSITY

Assessment of defoliation severity and extent was completed using the data product from Pasqurella *et al.* (2017) for years including 2015, 2016, and 2017. An example of the 2016 annual defoliation data product is shown in **Figure 6.** In this figure, defoliation intensity for each 250 by 250 meter raster pixel is based on the comparison of measured versus expected tasseled cap greenness values (Pasquarella *et al.*, 2017). More negative values identify locations of high defoliation intensity. Blue points show the locations of USGS stream gage sites, dark blue shows reference gage sites.

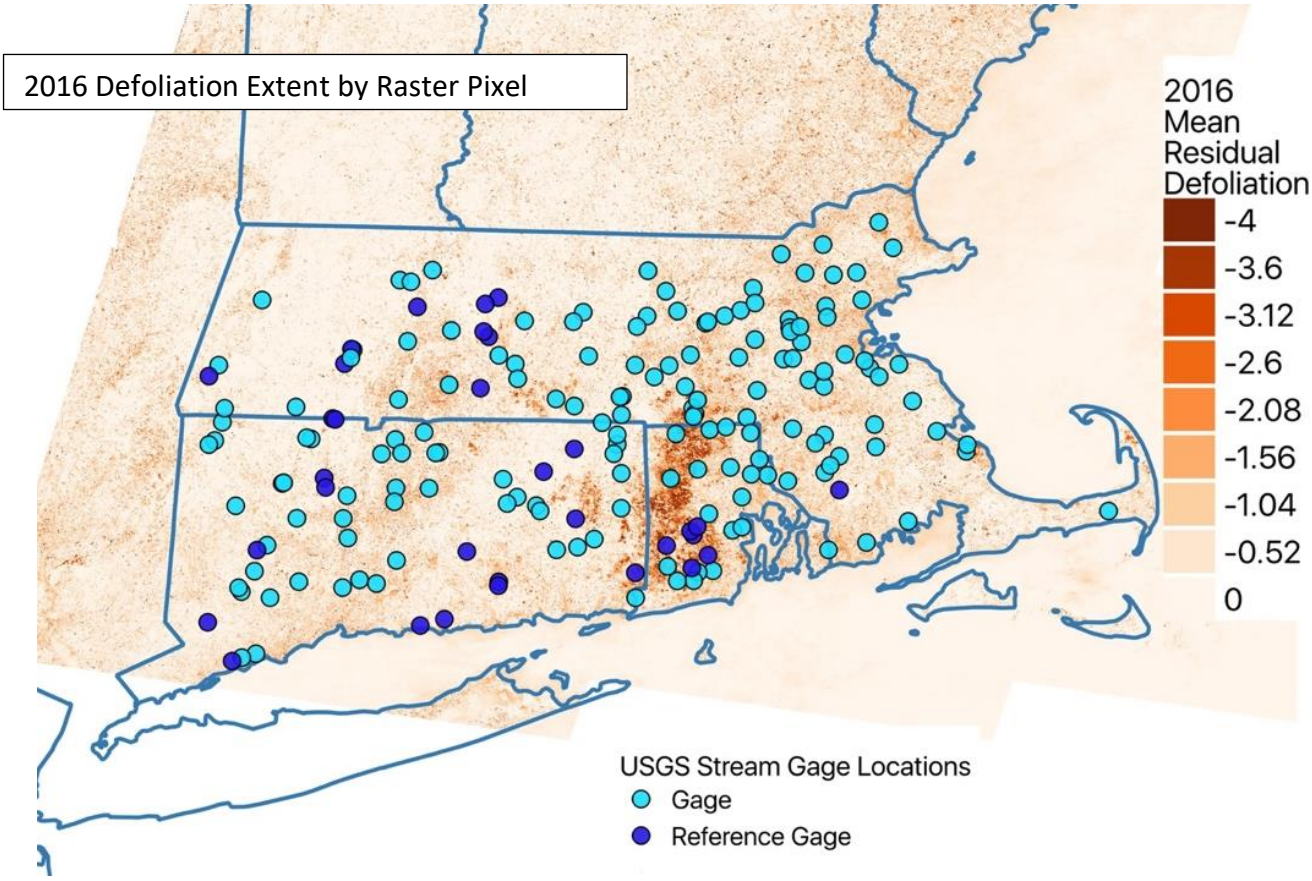

Figure 6:2016 Defoliation Extent from Landsat data with Locations of USGS Stream Gage Stations. Location of USGS stream gage study sites overlaid with output of Pasquerella et al. (2017) model for 2016 defoliation. Reference stream gages (Falcone, 2011) shown in dark blue. All USGS stream gages shown in light blue. Defoliation (a scale of light to dark brown) is the most intense when dark brown.

The 2016 (**Figure 6**) and 2017 defoliation (**Figure S1B**) were most intense in western Rhode Island and eastern Connecticut. **Figure 6** highlights the variable intensity of defoliation of the outbreak season and over the landscape extent that is apparent in 2015, 2016, and 2017 (**Figure 6, Figure S1**). Pixels with high levels of defoliation are often proximate to areas with medium to minimal defoliation (e.g. patches of low defoliation among areas intense defoliation of Southern Rhode Island). Reference and non-reference stream gages are located in areas across the spectrum of high and low defoliation values (**Figure 5**). Additionally, there are a select number of reference stream gages in southern Rhode Island, which had the most intense defoliation in 2016.

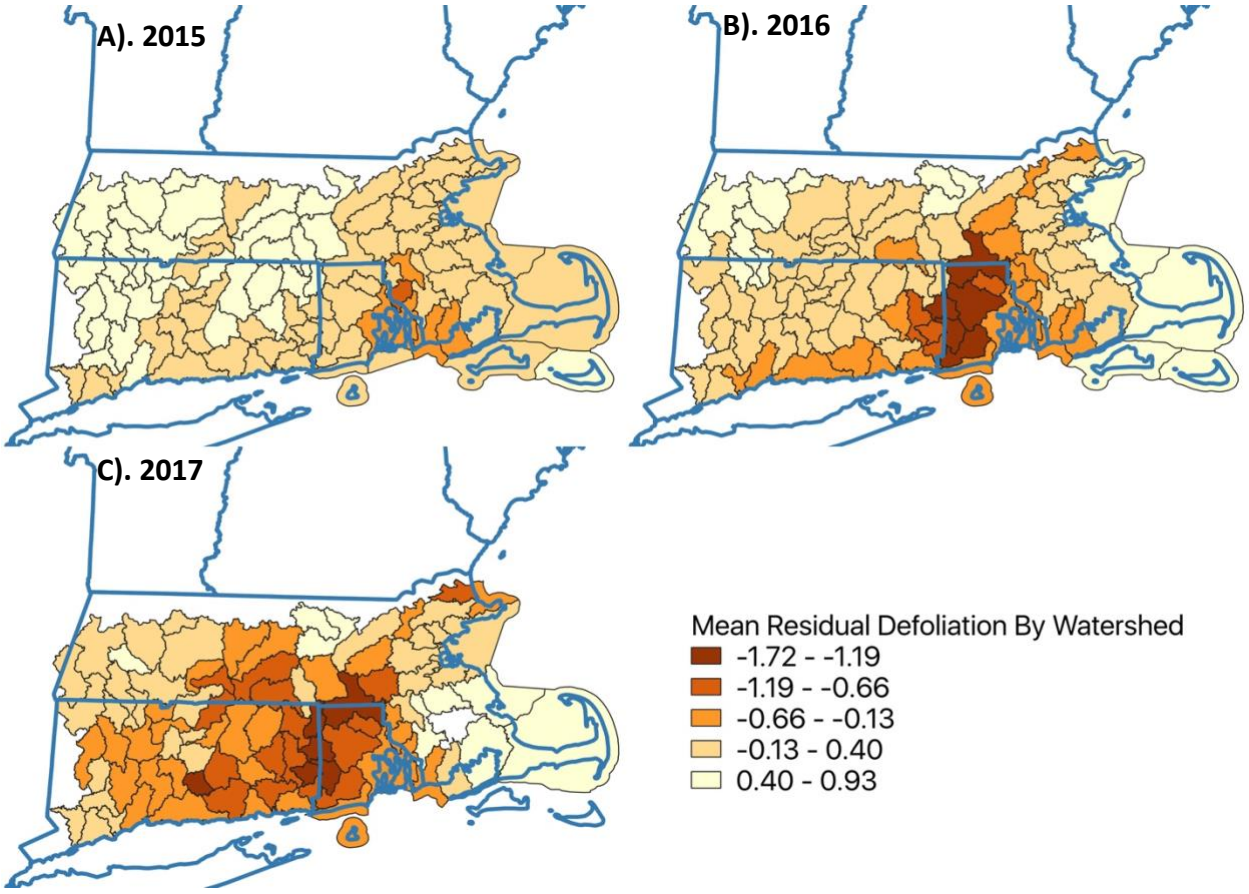

Figure 7: (A-C) Annual Mean Residual Defoliation By Watersheds (A – 2015; B – 2016; C – 2017) averages calculated using zonal statistics of annual defoliation partitioned by Watershed (Hydrologic Unit 01,10 digit or watershed scale). Color scale is the same in all years.

This spatial variability in defoliation is consistent in 2015, 2016 and 2017 (**Figure 7**, **Figure S1**). Defoliation was most intense in 2016 and most widespread in 2017. **Figure 7** shows the mean watershed defoliation value for 2015, 2016, and 2017 as calculated from the mean defoliation of all pixels in the watershed. Units are equal in all years. The highest mean values for defoliation occurred in 2016 when three watersheds in southern Rhode Island had mean defoliation values less than -1.19 (**Figure 7B**). The 2017 defoliation had a greater spatial extent compared to 2016: 21 watersheds had mean defoliation less than 0.66 compared to 10 watersheds in 2016 (**Figure 7**). In all years, defoliation is concentrated in western and southern Rhode Island as well as eastern Connecticut. In Connecticut and Rhode Island, four watersheds saw repeated intense defoliations in 2016 and then again in 2017. In these watersheds, mean-watershed defoliation was 1.19 to 1.72 standard deviations below the mean.

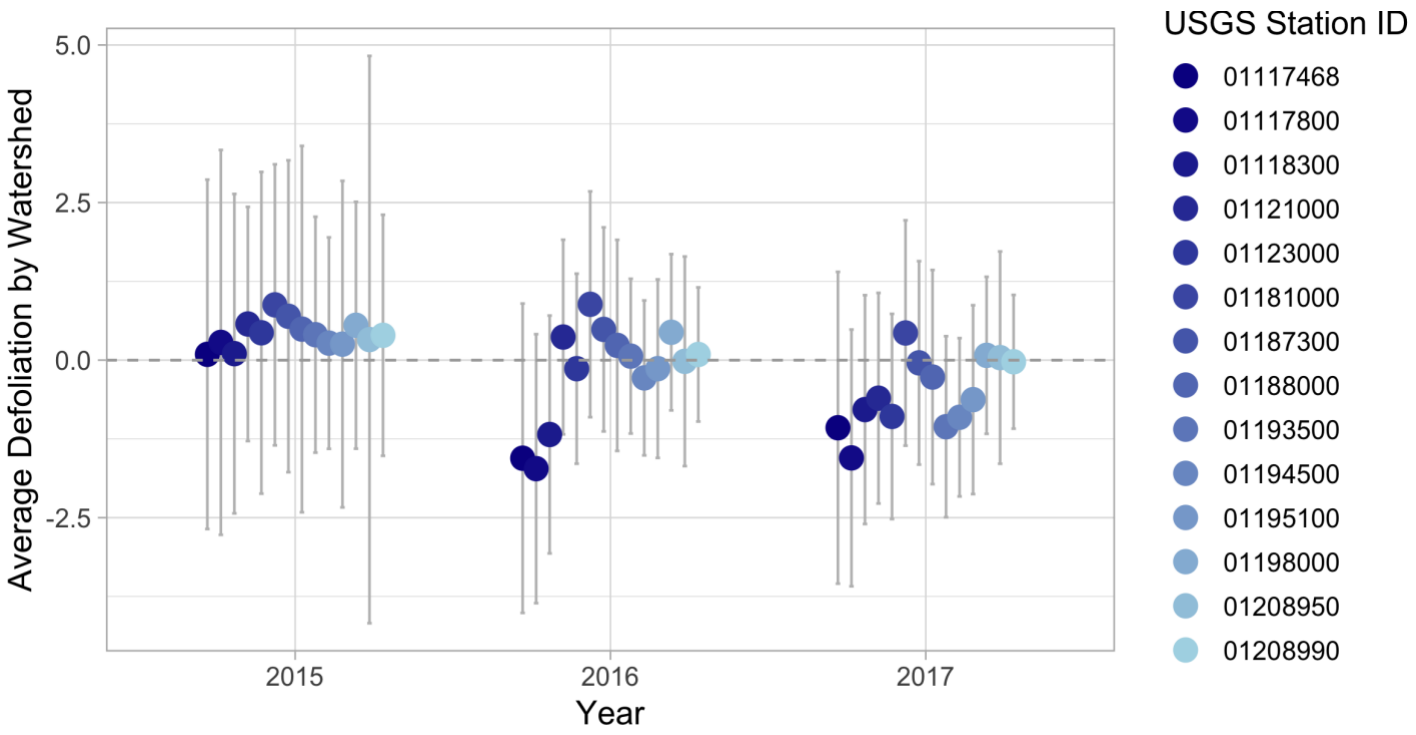

Figure 8 (A-C) Mean Residual Defoliation for watersheds of 16 reference USGS Stream Gages. Reference gages limited to those with more than 18 years of data 1998-2018. Dots represent mean for watershed, bars show standard deviation. The grey line represents line where difference from long-term greenness model is zero. Mean Residual produced from integrated Tasseled Cap Greenness model Mid-June through September (Pasquarella *et al.*, 2017). Watershed defined by Watershed Boundary Dataset for hydrologic unit code (HUC) 10-digit scale (USGS *et al.*, 2018).

Negative defoliation values at stream gage locations are correlated to a decrease from the 10-year greenness baseline. **Figure 8** shows the defoliation values of each watershed for reference stream gages during the 2015-2017 time period. Mean watershed level defoliation (where more negative values correlate to more intense defoliation) are plotted by year for each stream gages. Error bars represent one standard deviation of the averaged pixel values. Large standard deviations in defoliation across all years support the high variability and inconsistent defoliation patterns noted in **Figure 7**. **Figure 8** additionally shows the chronology of gypsy moth defoliation across the southern New England watershed landscape. In 2015, all 14 reference stream gages used in this study had positive average defoliation values. In 2016, five stream gages had negative mean defoliation values. In 2017, ten stream gages had negative

mean defoliation values. In all cases, high variability in defoliation suggests that watersheds were partially defoliated and there was large variation in defoliation intensity throughout the watersheds. The watershed with the most intense average defoliation values included reference stream gage ID #s 01117468, 011178000, 01118300, which are the reference stream gages of Southern Rhode Island noted in **Figure 6**.

3.2 Flow Values Among Years

Flow duration curves were used to assess flow regimes of individual years in comparison to baseline and among years. These curves plot the fraction of time that a specific flow magnitude (value) is exceeded. Flood events occur anywhere from 5% to 25% of the time and are represented as when flow exceeds a specific value. For example, a stream that is considered flooded when flows are greater than 15 m^3/s would have a flow duration curve which includes these flow values less than 25 % of the time.

Figure 9 show flow duration curves for each reference stream gage used in the study. Flow duration curves rank values of discharge based on the fraction of time that stream flow is above or equal to these values. The black lines show the long-term mean flow duration curve produced from stream discharge data from 1998 – 2018. Colored lines are by year and include years with defoliation data (2015 - green, 2016 - golden, 2017 – red). As reference gages have had little change in their watershed, baseline values (black) are considered representative of normal streamflow regimes. **Figure 9** shows flow duration curves for stream gages in order of defoliation intensity measured in the watershed either in 2016 and 2017. Different stream gage locations vary in daily discharge values (in m^3/s). The average flow ranges from 10^{-2} to 10^4 in m^3/s. Normal flow conditions, which occur 25 to 75% of the time are about 10 m^3/sec in most streams.

Flow duration curves in this study are typical in that low flow values are exceeded 95% of the time or more and high flow values are rare (McMahon *et al.*, 2003). Most flow duration curves for 2015 and 2016 are below baseline and 2017 data. In 2017, heavily defoliated watersheds are above baseline values (row 1, **Figure 9**) whereas less defoliated watersheds

overlap with baseline flow values (row 4, **Figure 9**). In 2017, more defoliated streams had higher flow values at high time proportions compared to the 20 -year baseline. These streams show positive deviance from baseline starting at time fractions greater than 0.25. Time fractions greater than 0.25 are representative of normal and low flow values.

In 2015 and 2016 eight streams had a distinct increase in the time fraction of high flow events compared to baseline flow (**Figure 9**). Both the most defoliated watershed (stream gage ID# 01117800) and the least defoliated stream (stream gage ID# 01181000) had an increase in time fraction with high flow events in comparison to the baseline flow. Overall, these increases in high flow events are at time fractions less than 0.25 and are apparent in streams with varying levels of defoliation.

In addition to characterizing flow using flow duration curves over 20-year and yearly timescales, other stream parameters were visually assessed. These stream parameters included the 7-day discharge, maximum daily discharge, mean-daily discharge, and standard deviation. Of the 89 streams assessed, 50 showed a decrease in maximum flow values and mean daily flow values during the months of May, June, July, and August (Data not included). This suggests that discharge in throughout stream gages gradually decreased over the past 20 years. These trends are important to incorporate into long-term analyses of flow changes. However, as this study is concentrated on analyses at an annual scale and no stream gages showed dramatic alterations, all stream gages are included in later analyses.

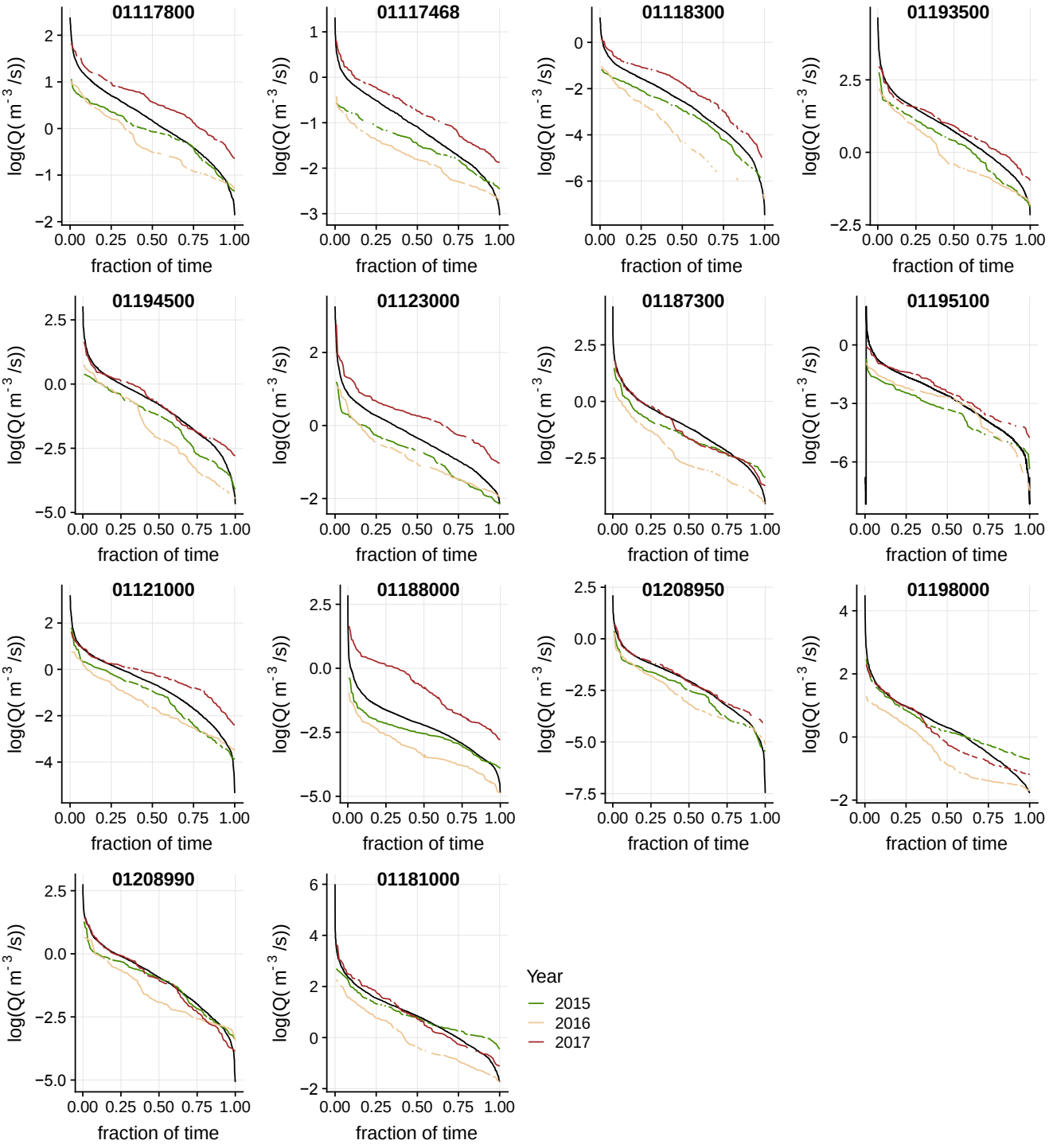

Figure 9: Flow Duration Curve for Reference Stream Gages in Decreasing Order of Mean Watershed Defoliation. Flow Duration curves are plotted for 1998 – 2018 (black), 2015 (green), 2016 (golden), 2017 (red). The x-axis shows the fraction of time stream exceeded the value of discharge (Q) in log units. Discharge converted from cubic feet per second (cfs) to m^3/s as averaged by day. Curves are ordered by the maximum defoliation value in measured in the watershed in either 2016 or 2017.

3.3 Precipitation Values At Stream Gage Locations

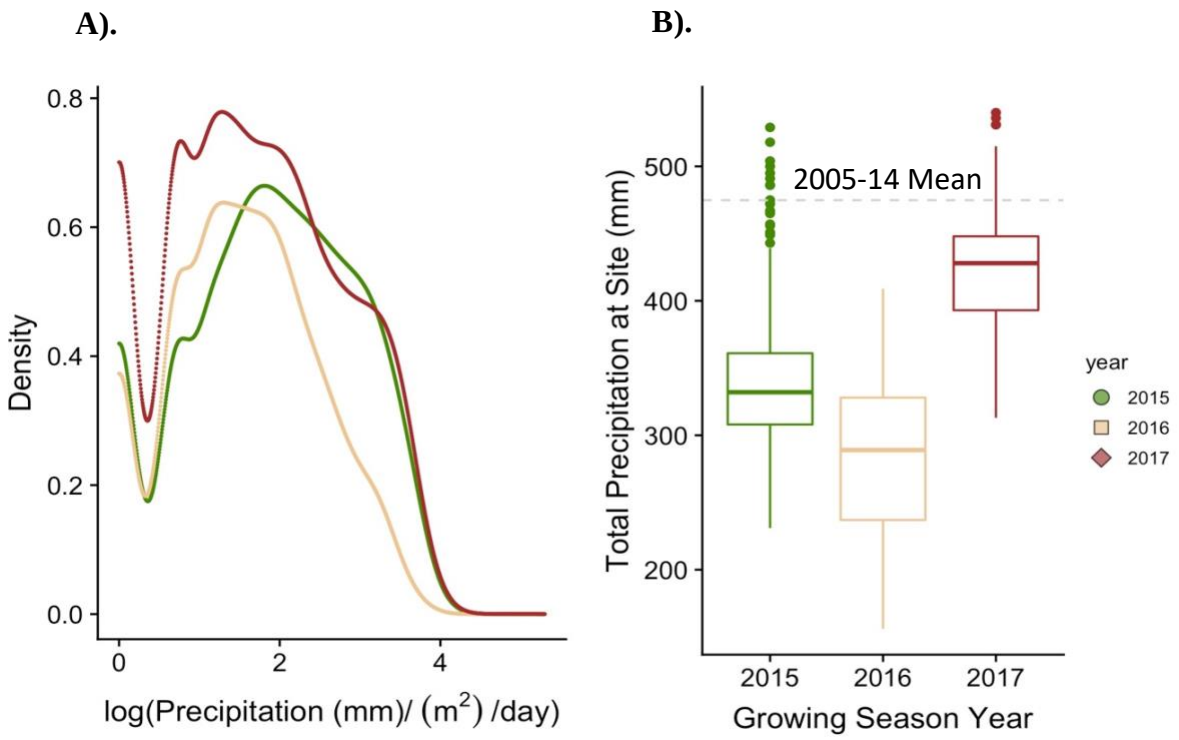

Figure 10: Daymet Precipitation for All Stream Gages in 2015, 2016, 2017. (A). Density curve of the log of precipitation in mm / m^2 per day for all stream gage locations. Value of each curve sums to the total precipitation measured for all stream gages sites by year **(B).** Total precipitation over the growing season in mm. Decadal mean from 2005-2014 is plotted in grey. Colors correspond to year, 2015 (green), 2016 (golden), 2017 (red).

The intensity of individual precipitation events varied by year. **Figure 10 (A)** is the distribution of precipitation values normalized to the total yearly rainfall (mm) during the growing season of 2015, 2016, and 2017. In this figure, zero precipitation values are omitted from the distribution. It is important to note zero values are the dominant measurement for all stream gages in all years. Of non-zero precipitation values 2015-2017, daily Daymet precipitation measurements ranged from 1mm to 159mm, with a mean of 9.79 and a standard deviation of 10.8mm. 2015 had a relatively low number of small precipitation events, with a higher proportion of precipitation measured during large events. 2016 had a higher proportion of small precipitation events relative to 2015, but precipitation deposition was dominated by

medium precipitation events. 2017 had the highest proportion of small precipitation events, dominated by medium size precipitation events (**Figure 10 A**).

Precipitation was highest in 2017, but was below the 10-year precipitation average for all stream gages. **Figure 10 (B)** is the total precipitation over the growing season (May-August) at each stream gage location. The midline of the boxplot represents the median of the data, and points above the boxes show outliers. In 2015, the median total precipitation for all stream gage locations was 332 mm. In 2016 the median value was 289 mm, and in 2017 the median value was 428 mm. In all years, the median precipitation value was less than the 10-year decadal mean of 475 mm (shown on the grey line, **Figure 10B**).

3.4 Discharge:precipitation Ratio With Defoliation

I analyzed variation in the ratio of watershed discharge to precipitation for all stream gages by fitting a linear model with mean watershed level defoliation and year as the independent variables (**Figure 11** A & C). Precipitation was aggregated from Daymet daily precipitation values at the location of each stream gage. The defoliation data product includes defoliation as the difference to the 10-year greenness baseline, where more foliation is positive, and more defoliation is negative. In **Figure 11**, I multiplied mean defoliation by -1 to more intuitively relate an increasing discharge: precipitation to increasing defoliation. Values of defoliation in all years ranged from -1 to 1.75 (where more positive values are increased defoliation). **Figure 11** includes the discharge-to-precipitation response for each stream gage in all **(A)** and reference **(C)** stream gages. The 2015 defoliation values are mostly negative, which indicates low defoliation in 2015 (also noted in **Figure 3**). The 2016 -2017 data show a wide range in defoliation values, where 2017 has defoliation values concentrated about 0 (**Figure 11 A**)**.**Discharge:precipitation in all stream gages ranged from 0.05 to 0.85, with a mean value of 0.36. For reference gages, the discharge:precipitation ranged from 0.11 to 0.68 with a mean of 0.35. In 2015, discharge:precipitation ranged from 0.09 to 0.60, with a mean 0.29. In 2016, values were similar (range 0.11 to 0.48, mean = 0.24). 2017 had higher mean discharge values ranging from 0.08 to 0.65 (mean = 0.41).

The discharge:precipitation ratio was affected independently by defoliation and year. 2015 (green) values are less defoliated centered on the range of discharge:precipitation when compared other years. 2016 (golden) values are lower than most discharge:precipitation values of 2015 and, in particular, those of 2017. 2017 values are consistently above values of the other two years. 2015 appears to have a negative slope. However, of the 87 stream gages in 2015, only 5 had negative mean defoliation. Thus the relationship described in 2015 is not an output of defoliated watersheds, but rather variation in the overall range of foliar density. The positive relationship between defoliation and discharge:precipitation is consistent between all and reference gages. However, reference gages show more scatter (shown in the grey area around the lines **Figure 11 C**)

To account for site-specific variation in discharge:precipitation, the residual discharge:precipitation values from the 10 year mean (2005-2014) discharge:precipitation was calculated (**Figure 11 B & D**). The residual value represents annual departure of discharge:precipitation from the site-specific 10-year mean. In these graphs, negative values are when that year's discharge:precipitation is less than the 10-year mean and positive values are when that year's discharge:precipitation is greater than the 10-year mean. Relationships among years are consistent with non-residual data. 2016 is consistently below the 10-year mean value, whereas 2017 is consistently above. 2015 are closer to site-specific means, but the majority are below the 10-year mean value (78 of 87 stream gages). To assess the significance of these relationships, I fit linear models to the data for each year. Similar to the directions of linear models in **Figure 11 A and B,** residual relationships also show a positive association between defoliation and higher discharge:precipitation (**Figure 11 B and D**).

The significance of variation was tested using an ANOVA of the linear model on changes in discharge:precipitation associated with watershed level defoliation and year. **Table 1** shows ANOVA test results where discharge:precipitation is a function of watershed-level defoliation and year. As the watershed area was used to calculate mean defoliation and precipitation, I fit a linear model to test for correlation between mean defoliation and watershed size. As expected, the results of this model were not significant ($p = 0.31$; SI Table 3). This allowed for the significance of variance associated with discharge:precipitation and defoliation and year to be

tested using an ANOVA test. Results of the ANOVA show that although 2015 appears to have a negative relationship with defoliation and discharge, the model rejects the hypothesis that the association between defoliation and discharge:precipitation differs by year. The ANOVA model supports a strong association between defoliation and discharge:precipitation in all and reference gages (**Table 1**). Variation by year also accounts for a significant proportion of variation in the discharge:precipitation data (**Table 1**). These patterns are consistent with the visual differences among years (**Figure 11 B and D**). However, the interaction between defoliation and year was not significant in reference and non-reference stream gages. This suggests that the relationship between defoliation and discharge:precipitation is consistently positive across all years and can be described by a linear model (**Table 1**).

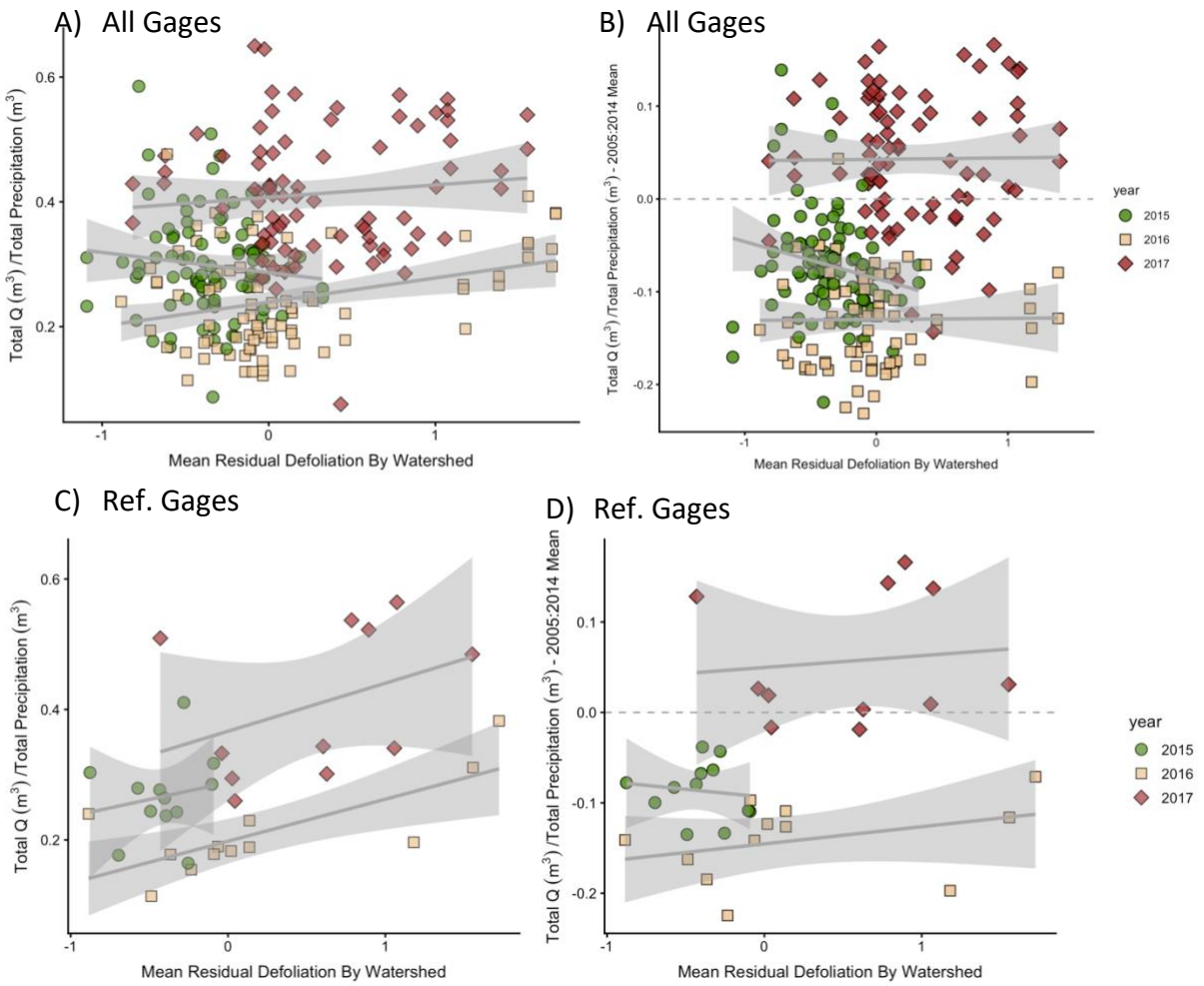

Figure 11: Mean discharge : precipitation ratio (A & C) and residuals mean discharge (B&D) from 8 year moving mean values for all stream gages (A-B) and reference gages (C-D). Residual values are calculated from a 10 year decadal mean. In all plots, a linear model with 95% confidence intervals (shown in gray) is reported for each year. Values for stream gages are colored and shaped by year (green circles – 2015, tan squares – 2016, red diamonds – 2017). Statistics of linear regressions included in **Table 1**.

Table 1: Mean defoliation as a function of residual Discharge:precipitation ratio and year for all and reference stream gages. Results of ANOVA of linear model show the coefficient estimate and respective significance values. Residual Discharge:precipitation ratio is calculated with a moving average with from a 10 year window. Residual Discharge:precipitation ratio and year are interaction terms.

		Dependent variable: Residual Discharge: Precipitation	
		(*All Gages*)	(*Reference Gages*)
Two-Way ANOVA	Mean Defoliation	F(1;249) = 22.13, p << 0.01	F(1;29) = 14.336, p << 0.01
	Year	F(2;249) = 169.86 p << 0.01	F(2; 29) = 36.998, p << 0.01
	Mean Defoliation * Year	F(2;249) = 2.20, p = 0.13	F(2; 29) = 0.14, p =0.847
Correlation Coefficient	Observations	255	35
	Adjusted R^2	0.587	0.711
	Residual Std. Error	0.059 (df = 249)	0.052 (df = 29)

3.5 Summary of Findings

Key results identified in the present study and to be discussed in conclusions and future work are as follows:

3.1 Defoliation intensity varies by year and by watershed

3.2 Flow regimes varied by year. Watersheds with high defoliation had increased flow at high time fractions.

3.3 Total precipitation was greatest in 2017, but all years were below the 2005-2014 mean. 2015 and 2016 had a number of large rain-events.

3.4 Discharge:precipitation is linearly related to defoliation and to year. The relationship of defoliation and discharge:precipitation is not altered by year

4. Discussion and Conclusions

4.1 Defoliation Extent and Intensity

Our analyses found that defoliation intensity varied within and among watersheds in 2016 and 2017, and that some watersheds had substantially lower mean defoliation values when compared to long-term mean conditions (**Figure 8**). Levels of defoliation measured in watersheds within this study ranged from no defoliation to 1.75 standard deviations below the long-term greenness baseline. Compared to USGS aerial sketch results, model values less than the long-term greenness baseline are generally associated with moderate to severe defoliation or 10 – 50% forest defoliated (Pasquerella *et al.*, 2017). Values -1 and greater standard deviations below baseline are associated with a 30- 50% canopy reduction. In our study, three watersheds had multiple years of moderate to high-intensity defoliation at a watershed scale (**Figure 8),** which could be compared to a selectively logged paired-catchment studies (Brown *et al.*, 2005; Bosch and Hewlett, 1982).

2016-2018 was the most intense defoliation event in New England since 1981, however sequential high-intensity defoliation events are common in the oak forests that dominate southern New England (Elkington and Boettner, 2016; Morin and Liebhold, 2016; Kegg, 1972;). Aerial survey maps show that areas of southern New England had over 12 years with defoliation from 1975 through 2010 (Morin and Liebhold, 2016). The oak-hickory forest type is the preferred gypsy moth foraging plant. As such, it is about ten times more likely to experience three successive years of defoliation compared to all other forests types (Ruefenacht *et al.*, 2008; Morin and Liebhold, 2016; Liebhold et al., 1992). Prior estimates of defoliation outbreak cycles have found a periodicity in outbreaks of 4-5 years in oak-hickory forests and 8-10 years in other forest types (Johnson *et al.*, 2006). Considering this cycle, southern New England is above average. Typical gypsy moth population cycles would result in 7 outbreaks during a 35-year time period compared to the observed 12 outbreaks or more (an outbreak every 2-3 years).

Areas of Southern Rhode Island and eastern Connecticut that experienced the highest intensity defoliation in 2016 and 2017 also have a legacy of defoliation events (Morin and Liebhold, 2016; **Figure 7**). This is likely related to the high proportion of susceptible and

contiguous oak-hickory forests in these areas (Davidson *et al.*, 1999; Ruefenacht *et al.*, 2008). Importantly, these successive years of defoliation are known to cause a nearly exponential increase in oak tree mortality. Mortality rates of trees post-defoliation are highly site-specific, and increase upon repeated defoliation. After the first year of defoliation, oak species mortality rates range from 1- 6.5 %, but after the fourth year mortality rates range from 3.5 to 63 % (Kegg, 1972; Morin and Liebhold, 2016).

Increased drought frequency in the northeast threatens to increase the scale and frequency of gypsy moth outbreaks(Hayhoe *et al.*, 2007). The majority of gypsy moth outbreaks in southern New England occurred prior to the establishment of the *Lymantria disparnucleovirus* and *Entomophaga maimaiga* which have dramatically decreased the frequency and intensity of gypsy moth defoliation events (Morin and Liebhold, 2016). The 2016 -2018 outbreak overlapped with areas of high oak populations and areas with a legacy of outbreaks and multi-year defoliation (Morin and Liebhold, 2016; Ruefenacht *et al.*, 2008; **Figure 7**).

A legacy of disturbance has existed in Northeastern forests since and prior to Euroamerican settlement , but increased gypsy moth disturbance, like that shown in 2016-2017, suggest watershed scale changes in forest composition are occurring to this day. Since Euroamerican settlement, southern New England forests have experienced a broad decline in oak species (a nearly 37% decrease). Chestnut, beech, and oak species have decreased in abundance while less drought tolerant maple species have increased (Nowacki and Abrams., 2015). The literature is not conclusive on oak emergence post gypsy moth-related tree mortality events (Nowacki and Abrams, 2015; Morin and Liebhold, 2016). Shifts in climate in conjunction with these changes in forest composition and the increasing likelihood of gypsy moth disturbance could enhance the risk of a large-scale forest composition change over decadal scales.

4.2 Flow Duration Curves

Flow duration curves were used to assess characteristics of flow regimes in 2015, 2016, and 2017 compared to baseline streamflow regimes. I limited my flow duration curve analyses

to USGS reference stream gages, as the patterns in flow duration curves are heavily influenced by the relative amount of impervious surface in the watershed (Dingman, 2015; McMahon *et al.*, 2013). I found that streams with higher levels of defoliation in 2017 showed a pattern of higher flow values at a greater fraction of the time as compared to baseline and prior years (**Figure 9**). 2015 and 2016 had overall flow rates that were below baseline, but this was expected due to the 2015 and 2016 drought (NOAA, accessed April 17th, 2019).

In comparison to baseline, eight stream gages in 2017 had an increase **in** the discharge amount at normal and low flow time values. These streams are also located in watersheds with high amounts of defoliation (**Figure 9**). Flow duration curves of more defoliated watersheds were also well above 20-year baseline values, while precipitation in the region was still below the 10-year average (**Figure 9; Figure 10**). Increased amounts of time above baseline flow has been observed in logged forests and in urbanized stream catchments. A paired-catchment study at Hubbard Brook, an experimental forest in the White Mountains of New Hampshire, mirrored the pattern shown in **Figure 9** and hypothesized in **Figure 5**. This study found that the water yield during the growing season increased after logging and that there was higher streamflow at greater proportions of time compared to a model of non-affected flow (Hornbeck *et al.*, 1997). Similarly, a study in urbanized watersheds found urban development increased the duration and frequency of higher flow conditions (McMahon *et al.*, 2003). Urban development is associated with decreased forest cover and increased impervious land area, decreasing evapotranspiration in a way that is similar to that of gypsy moth defoliation (McMahon *et al.*, 2003; Clark *et al.*, 2012).

The pattern of increased duration of higher flow values observed in paired-catchment studies, urbanized streams, and defoliated streams are inverse to the patterns of afforested flow duration curves. A paired water catchment study of afforested watersheds found low flow values occurred a higher proportion of time when compared to the non-forested paired catchments (Brown *et al.*, 2013). This study reasoned that the inverse pattern of afforested watersheds was a result of summer evapotranspiration exceeding rainfall. Increases in evapotranspiration from afforestation decreased discharge at the stream-site, and caused already low summer discharge values to become lower (Brown *et al.*, 2013). Following this, my

results for defoliation (as opposed to afforestation) suggests that with repeated defoliation summer evapotranspiration is lower than baseline values. This decrease in evapotranspiration causes normally low summer discharge values to become higher, and increases the proportion of time at higher flow values. (**Figure 9**).This conclusion recommends that future work investigate if changes in evapotranspiration are also detectable in flow duration curves from flow values of other seasons. This work would help understand how and if discharge is changed following a defoliation event.

This study did not find that high flow flood events increased in magnitude with defoliation. The greatest deviation from baseline and prior years' flow during defoliation occurred 75% of the time or more. 75% percent of the time or more is representative of normal to low streamflow values (**Figure 9**). Flood events are defined anywhere from 5% to 25% of the time or less. In 2015 and 2016, the flow duration curves of eight stream gages had distinct increases in the proportion of high flows. However, this pattern is observed across a range of defoliation values and we thus conclude that these events are not related to the extent of defoliation in the watershed (Figure 9). This is contrary to the findings in Hubbard Brook, where the magnitude of flood events increased deforested watersheds (Hornbeck *et al.*, 1997).

Instead of relating increases in high flow noted 2015 and 2016 to defoliation, we instead conclude they are likely related to an increased proportion of high-intensity rain events compared to baseline and 2017 (Figure 9). Prior work on flow duration curves and high flow or flood events found that the duration and frequency of these events are best represented by the morphology of the stream channel and the characterization of the precipitation event itself (McMahon *et al.*, 2003). At an annual time scale, changes in stream channel morphology are unlikely. Instead, an increased frequency of high-precipitation events likely increased the frequency of high flow values (**Figure 9 and 10**) The high-intensity and stochastic precipitation events during 2015 and 2016 would increase the number of high stream flow periods because rapid water flux into the watershed would also have rapid water flux out of the watershed (Dingman, 2015).

Our analyses support an increase in the proportion of high flow events in 2015 and 2016 that are related to high-intensity precipitation events, and 2017 increased normal and low

flow discharge values are associated with defoliated streams. We saw greatest deviance from baseline at time fractions greater than 75% of the time, representing normal and low flow values. In our analyses, high flow discharge values showed little variation or shift likely because the frequency and peakedness of a high flow event are mostly related to the stream morphology and precipitation, which are not directly influenced by evapotranspiration on a short time scale.

4.3 DISCHARGE:PRECIPITATION

The discharge:precipitation ratio was used to quantify the proportion of water draining from the watershed above the stream gage. Years with defoliation had a positive relationship between defoliation and discharge:precipitation (**Figure 11**). Differences in these ratios suggest changes in evapotranspiration and interception where:

$$\Delta \frac{Discharge\ \left(\frac{m^3}{year}\right)}{Volume\ Precipitation\left(\frac{m^3}{year}\right)} \propto -\Delta(\mathrm{Q}_{evapotranspiration} + \mathrm{Q}_{interception})$$

Theoretically, increases in discharge:precipitation ratios are the result of decreases in evapotranspiration and interception. Our study found that there was an increase in discharge:precipitation in defoliated years and that this relationship exists when site-specific variation was taken into account through the calculation of the residual discharge:precipitation from a decadal mean (**Figure 11** A and C *vs*. B and D). My findings supported that increases in discharge:precipitation are well described by a linear relationship. This relationship is particularly well fit in reference gages, which are less impacted by other anthropogenic disturbances or trends (*Reference gages* R^2*:* 0.711 $F(1;29) = 14.336$, $p << 0.01$). The relative effect of defoliation on discharge:precipitation was greatest in 2016 when defoliation was most severe and watersheds with the highest mean defoliation had an estimated 30-50% canopy cover loss.

A 30-50% reduction in canopy cover has been well documented to increase water yield in many different forest types (Bosch and Hewlett, 1982; Brown *et al.*, 2005; Hornbeck *et al.*, 1997). In these studies, the extent of canopy removal is associated with a 100-300 mm increase

in watershed water yield. The present study did not directly estimate water yield for the different stream catchments, and as a result is not able to directly compare values among water yield and discharge:precipitation. The present did find a significant association between defoliation and discharge:precipitation apparent in all years. Such increases in discharge have also been supported by work with stream gages in defoliated watersheds of southern New England. One study of a stream gage in Rhode Island compared 2015 and 2016 discharge and found discharge was five times greater during a defoliated year (Addy *et al.*, 2018). Given that precipitation between the two years was similar among most stream gage sites, the combination of my study results with this single stream gage analysis indicates that large discharge increases are associated with defoliation. These increases in discharge make sense in light of prior studies supporting rates of evapotranspiration decreased following a gypsy moth outbreak in oak and pine forests (Clark *et al.*, 2014). Thus, in relation to the second objective of this study, which asks if defoliation scales to discharge alterations, defoliation intensity is linearly related to increases in the volume of discharge in proportion to precipitation at most stream gage locations.

Our results support that defoliation is measurable at a watershed scale, and that discharge flows are altered by defoliation. Increases in discharge are most different from baseline during normal to low flow conditions and are not observed during large flow events (Figure 9). Increases in discharge are linearly related to increases in defoliation (Figure 11). Thus, this study concluded that defoliation is associated with alterations in stream flow and increases in stream discharge over both seasonal and daily time periods at a regional scale. These increases in the water flux out of the ecosystem could have important feedbacks for both ecosystem resilience and downstream water quality.

4.4 Broader Implications

4.4.1 Forest Composition

The repetition of disturbance and increased northeastern drought frequency will likely contribute to oak mortality and watershed-scale oak decline (Nowacki and Abrams, 2015). First, the intense defoliation that occurs at a watershed scale over multiple years is associated with

high tree mortality (Kegg, 1972; Morin and Liebhold, 2016). Oak-pine and mixed hardwoods of southern New England systems are adapted to periodic disturbances like high wind events, fire, and periodic forest insect infestations, but intense and more frequent disturbances put the steady-state nature of these ecosystems at risk (Nowacki and Abrams, 2015). Oak succession in the northeast has caused an increase in beech and maple forest types (Lovett et al 2016; Nowacki and Abrams, 2015). Oaks are the preferred host of gypsy moths, but they feed on many different deciduous trees, all of which have relatively high rates of transpiration (Liebhold *et al.*, 1992).

4.4.2 Sedimentation rates and habitat sustainability

A sustained increase in discharge that occurs during moderate to high-intensity defoliation could have important ecosystem and management implications. Increases in stream discharge can alter the habitat suitability of streams, as well as the rate of sediment transport. Work on fire disturbance in the Pacific Northwest has shown that fire increases watershed yield and sediment deposition (there are reports of post-fire sediment waves greater than >1m thick; Reeves *et al.*, 1995). Increases in sediment flux have dramatic implications for stream biota, and habitat quality (Dingman, 2015). Some studies have found that increases in stream discharge can have a positive effect on the biodiversity of stream biota, but can negatively impact specific species that require high water clarity (e.g. *Oncorynchus* species in the Pacific Northwest; Reeves *et al.*, 1995; Beudert *et al.*, 2015). Prior work in pine-beetle disturbed forests work has shown that increased erosion associated with increased discharge can decrease tree root strength, causing additional tree loss (Perry *et al.*, 2008). An overall decrease in root strength and high tree mortality increases the risk of landslide events (Perry *et al.*, 2008; Reeves *et al.*, 1995). In the Northeast's thin soil horizons, increased erosion could create changes in the long-term slope and habitat sustainability (Easton *et al.*, 2007).

4.4.3 Forest and water nutrient cycling

Future research could address implications of increased discharge and leaf loss on the short and long-term nutrient cycling, which are critical for forest ecosystems and freshwater resources (Barnes *et al.*, 2009). Recent work on a small watershed in Rhode Island found defoliation was correlated to increases in stream water temperature (values during defoliation

were consistently above 10-year stream temperature values), decreases in dissolved oxygen, and dramatic increases in nitrogen and phosphorous loading (Addy *et al.*, 2018).

Alterations in nitrogen and phosphorous loading following defoliation or other insect infestations have been documented worldwide (Beurdert *et al.*, 2015; Eshelman *et al.*, 1998). A 1998 study found that variations in streams' dissolved nitrogen flux in the 1980s through the 1990s were synchronized with gypsy moth defoliation events (Eshelman *et al.*, 1998). Additionally, the nitrogen composition of leaves after defoliation has been shown to decrease, suggesting an increase in leaf litter and runoff (Clark *et al.*, 2014). Nitrogen and phosphorous fluxes are important parameters for biologic productivity and the resulting water quality (Barnes *et al.*, 2009).

Northeastern canopies are reliant on healthy ecosystem cycling including nitrogen content of foliage. Following a disturbance, nitrogen flux in streams increases and nitrogen content in new leaf foliage decreases (Beudert *et al*., 2015; Addy *et al.,* 2018; Clark *et al*., 2014). Post defoliation reduction in leaf nitrogen content was long-term, suggesting that recovery of lost nitrogen content is slow (Clark *et al.,* 2014). As most North American forests are nitrogen limited (nitrogen is considered a limiting factor of total ecosystem productivity), long-term reductions nitrogen availability caused by leaf loss and discharge flux could have important implications for the resiliency of a forest ecosystem (Driscoll *et al.,* 2003).

Nitrogen is also an important determinant of downstream water quality. Nitrogen has previously been identified as one of the key pollutants in the Northeast (Driscoll *et al*., 2003). Increases in flux of reactive forms of nitrogen are linked to decreased pH, which alters the availability of some pollutants. Additionally, nitrogen flux in the northeastern United States has been strongly linked to coastal eutrophication (Driscoll *et al*., 2003). Understanding how defoliation alters water cycling and nutrient cycling is important for equal understanding of how overall ecosystem functioning is altered by a disturbance event.

4.5 Conclusions

Increasing drought frequency will likely increase frequency of defoliations, which will, in turn, increase the rate of spread to areas currently not affected by gypsy moths (Liebhold *et al*.,

1992; Davidson *et al.,* 1989; Hayhoe *et al.,* 2007). Gypsy moths currently inhabit only one-quarter of their potential US range (Liebhold *et al.*, 1992). In areas that are not adjusted to gypsy moth defoliations, new-defoliations can cause forest composition altering disturbance (Schweitzer *et al.*, 2014). Forest composition and widespread tree mortality have created an increase in discharge, but the duration of this increase is contested (Hornbeck *et al.*, 1997; Beudert et. al., 2015). Studies of mountain pine beetle disturbances have shown that tree mortality due to pine beetle disturbance causes long-term increases in the proportion and amount of groundwater measured in a stream (Bearup *et al.*, 2014; Reed *et al.*, 2018; Wehner and Stednick, 2017). Data from Hubbard brook showed a one-year increase in water yield, but, once forest regrowth was established, there were decreases in discharge that continued for an undetermined time-period (Hornbeck *et al.*, 1997). Increased discharge is advantageous for ensuring adequate water-supply and increased biodiversity, but defoliation can dramatically shift the long-term forest community (Schweitzer *et al.*, 2014; Hornbeck *et al.*, 1997; Beudert *et al.*, 2015; Swanson *et al.*, 2011). Watersheds with repeat and or newly introduced gypsy moth outbreaks that cause high tree mortality could, in turn, impact the forest canopy and associated water availability.

This study supported the conclusion that defoliation increased stream discharge in proportion to site-specific precipitation during the growing season across a regional network of stream gages. Daily changes in stream discharge depart from baseline most significantly during low-flow conditions (Figure 10). Differences in discharge:precipitation among individual stream-gages show that between 2015 and 2016 (which had similar levels of precipitation), discharge:precipitation ratios increased in defoliated watersheds. Southern New England has a legacy of gypsy moth defoliations and these events continue to have important implications for the stream water balance during and immediately following defoliation. Additionally, given the likelihood of increased defoliation with increased drought, there is a risk of alterations in long-term stream function (channel size, stream biota). This study recommends that those living and researching in areas newly affected by gypsy moth or other insect defoliations research how this could alter ecosystem watershed balances and the associated forest community.

In relation to hypothetical relationships described in **Figure 4**, this study has found there are increases in runoff and groundwater into streams following defoliation. This study recommends future research address how disturbance alters flux of critical nutrients and sediment. These fluxes can, in turn, shift the aquatic and terrestrial plant community as well as downstream water quality. This is knowledge is necessary to build an adequate understanding of how defoliation will impact ecosystem functioning and water resources.

REFERENCES

Addy, K., Gold, A.J., Loffredo, J.A., Schroth, A.W., Inamdar, S.P., Bowden, W.B., Kellogg, D.Q., and Birgand, F. (2018). Stream response to an extreme drought-induced defoliation event. *Biogeochemistr*y 140, 199–215.

Barnes, M., Todd, A., Lilja, R.W., and Barten, P. (2009). Forests, Water and People: Drinking water supply and forest lands in the Northeast and Midwest United States, June 2009. *United States Forest Service*

Bearup, L.A., Maxwell, R.M., Clow, D.W., and McCray, J.E. (2014). Hydrological effects of forest transpiration loss in bark beetle-impacted watersheds. *Nature Climate Change 4*, 481–486.

Beudert, B., Bässler, C., Thorn, S., Noss, R., Schröder, B., Dieffenbach-Fries, H., Foullois, N., and Müller, J. (2015). Bark Beetles Increase Biodiversity While Maintaining Drinking Water Quality. *Conservation Letters 8*, 272–281.

Bosch, J.M., and Hewlett, J.D. (1982). A review of catchment experiments to determine the effect of vegetation changes on water yield and evapotranspiration. *Journal of Hydrology 55*, 3–23

Brown, A.E., Zhang, L., McMahon, T.A., Western, A.W., and Vertessy, R.A. (2005). A review of paired catchment studies for determining changes in water yield resulting from alterations in vegetation. *Journal of Hydrology 310*, 28–61

Brown, A.E., Western, A.W., McMahon, T.A., and Zhang, L. (2013). Impact of forest cover changes on annual streamflow and flow duration curves. *Journal of Hydrology 483*, 39–50.

Clark, K. L., Skowronski, N., Gallagher, M., Renninger, H., & Schäfer, K. (2012). Effects of invasive insects and fire on forest energy exchange and evapotranspiration in the New Jersey pinelands. *Agricultural and Forest Meteorology, 166*, 50-61.

Clark, K. L., Skowronski, N. S., Gallagher, M. R., Renninger, H., & Schäfer, K. V. R. (2014). Contrasting effects of invasive insects and fire on ecosystem water use efficiency. *Biogeosciences, 11*(23), 6509-6523.

Davidson, C.B., Gottschalk, K.W., and Johnson, J.E. (1999). Tree Mortality Following Defoliation by the European Gypsy Moth (Lymantria dispar L.) in the United States: A Review. *Forest Science 45*, 74–84.

Dietze, M.C., and Matthes, J.H. (2014). A general ecophysiological framework for modelling the impact of pests and pathogens on forest ecosystems. *Ecology Letters 17*, 1418–1426.

Dingman, S.L. (2015). *Physical Hydrology: Third Edition* (Waveland Press).

Doane, C. C., & McManus, M. L. (Eds.). (1981). *The gypsy moth: research toward integrated pest management* (No. 1584). US Department of Agriculture.

Driscoll, C.T., Whitall, D., Aber, J., Boyer, E., Castro, M., Cronan, C., Goodale, C.L., Groffman, P., Hopkinson, C., Lambert, K., et al. (2003). Nitrogen Pollution in the Northeastern United States: Sources, Effects, and Management Options. *BioScience 53*, 357–374.

Easton, Z.M., Gerard-Marchant, P., Walter, M.T., Petrovic, A.M., and Steenhuis, T.S. (2007). Hydrologic assessment of an urban variable source watershed in the northeast United States. *Water Resources Research 43*, W03413.

Elkinton, J.S. & Boettner, J. (2016) Gypsy moth outbreak of 2016. *Massachusetts Wildlife Magazine, No. 3*

Elkington J.S., & Liebhold A.M. (1990). Population Dynamics of Gypsy Moth In North America. *Annual Review of Entomology. 35*(1), 571-596

Eshleman, K. N., Morgan, R. P., Webb, J. R., Deviney, F. A., & Galloway, J. N. (1998). Temporal patterns of nitrogen leakage from mid-Appalachian forested watersheds: Role of insect defoliation. *Water Resources Research, 34*(8), 2005-2016.

Falcone, J.A. (2011). GAGES-II: Geospatial Attributes of Gages for Evaluating Streamflow (Reston, VA: U.S. Geological Survey).

Kegg, J.D. (1973). Oak Mortality Caused by Repeated Gypsy Moth Defoliations in New Jersey. *Journal of Economic Entomology 66*, 639–641.

Hayhoe, K., Wake, C.P., Huntington, T.G., Luo, L., Schwartz, M.D., Sheffield, J., Wood, E., Anderson, B., Bradbury, J., DeGaetano, A., *et al.* (2007). Past and future changes in climate and hydrological indicators in the US Northeast. *Climate Dynamics 28*, 381–407.

Hicke, J.A., Allen, C.D., Desai, A.R., Dietze, M.C., Hall, R.J., Hogg, E.H. (Ted), Kashian, D.M., Moore, D., Raffa, K.F., Sturrock, R.N., *et al.* (2012). Effects of biotic disturbances on forest carbon cycling in the United States and Canada. *Global Change Biology 18*, 7–34.

Hirsch, R.M., and De Cicco, L.A., 2015, User guide to Exploration and Graphics for RivEr Trends (EGRET) and dataRetrieval: R packages for hydrologic data (version 2.0, February 2015): *U.S. Geological Survey Techniques and Methods book 4*, chap. A10, 93 p., https://dx.doi.org/10.3133/tm4A10.

Hoover, K., Grove, M., Gardner, M., Hughes, D.P., McNeil, J., and Slavicek, J. (2011). A Gene for an Extended Phenotype. *Science 333*, 1401–1401.

Hornbeck, J.W., Martin, C.W., and Eagar, C. (1997). Summary of water yield experiments at Hubbard Brook Experimental Forest, New Hampshire. *Canadian Journal of Forest Research. 27*, 2043–2052.

Huntington, T. G., Richardson, A. D., McGuire, K. J., & Hayhoe, K. (2009). Climate and hydrological changes in the northeastern United States: recent trends and implications for forested and aquatic ecosystems. *Canadian Journal of Forest Research, 39*(2), 199-212.

Johnson, D.M., Liebhold, A.M., and Bjørnstad, O.N. (2006). Geographical Variation in the icity of Gypsy Moth Outbreaks. *Ecography 29*, 367–374

Kendall, C., and McDonnell, J.J. (2012). *Isotope Tracers in Catchment Hydrology* (Elsevier).

Kim, J., Hwang, T., Schaaf, C.L., Orwig, D.A., Boose, E., and Munger, J.W. (2017). Increased water yield due to the hemlock woolly adelgid infestation in New England. *Geophysical Research Letters 44*, 2327–2335

Liebhold, A. M., Gottschalk, K. W., Luzader, E. R., Bush, R., & Twardus, D. B. (1997). Gypsy moth in the United States: an atlas. Gen. Tech. Rep. NE-233. Radnor, PA: US Department of Agriculture, Forest Service, Northeastern Forest Experiment Station. 36 p., 233.

Liebhold, A.M., Halverson, J.A., and Elmes, G.A. (1992). Gypsy Moth Invasion in North America: A Quantitative Analysis. *Journal of Biogeography 19*, 513–520

Lovett, G. M., Weiss, M., Liebhold, A. M., Holmes, T. P., Leung, B., Lambert, K. F., ... & Wildova, R. (2016). Nonnative forest insects and pathogens in the United States: impacts and policy options. *Ecological Applications, 26*(5), 1437-1455.

McMahon, G., Bales, J.D., Coles, J.F., Giddings, E.M.P., and Zappia, H. (2003). Use of stage data to characterize hydrologic conditions in an urbanizing environment. *Journal of American Water Resources Association 39*, 1529–1546.

Millar, C.I., and Stephenson, N.L. (2015). Temperate forest health in an era of emerging megadisturbance. *Science 349*, 823–826

Morin, R. S., & Liebhold, A. M. (2015). Invasive forest defoliator contributes to the impending downward trend of oak dominance in eastern North America. *Forestry, 89*(3), 284-289.

Moore, R.B., Jefferson, F., Stevens, W.C., and Frank, L. E., (1978). Ecological and economic effects of gypsy moth on watersheds, wildlife, and forest fire hazard. Essex Marine Laboratory, Essex, Conn. (In Press).

NOAA National Centers for Environmental information, Climate at a Glance: Statewide Time Series, published April 2019, retrieved on April 17, 2019 from https://www.ncdc.noaa.gov/cag/

Nowacki, G.J., and Abrams, M.D. (2015). Is climate an important driver of post-European vegetation change in the Eastern United States? *Global Change Biology 21*, 314–334.

Pasquarella, V., Bradley, B., Woodcock, C., Pasquarella, V.J., Bradley, B.A., and Woodcock, C.E. (2017). Near-Real-Time Monitoring of Insect Defoliation Using Landsat Time Series. *Forests 8,* 275.

Perry, D. A., Oren, R., & Hart, S. C. (2008). *Forest ecosystems*. JHU press.

Reed, D.E., Ewers, B.E., Pendall, E., Frank, J., and Kelly, R. (2018). Bark beetle-induced tree mortality alters stand energy budgets due to water budget changes. *Theoretical and Applied Climatology 131,* 153–165.

Reeves, G. H., Benda, L. E., Burnett, K. M., Bisson, P. A., & Sedell, J. R. (1995). A disturbance-based ecosystem approach to maintaining and restoring freshwater habitats of evolutionarily significant units of anadromous salmonids in the Pacific Northwest. In *American Fisheries Society Symposium.* 17, 334-349.

Ruefenacht, B., Finco, M. V., Nelson, M. D., Czaplewski, R., Helmer, E. H., Blackard, J. A., Holden, G.R., Lister, A.J., Salajanu, D., Wyerman, D., & Winterberger, K. (2008). Conterminous US and Alaska forest type mapping using forest inventory and analysis data. *Photogrammetric Engineering & Remote Sensing, 74(*11), 1379-1388.

Rustad, L., Campbell, J., Dukes, J.S., Huntington, T., Lambert, K.F., Mohan, J., and Rodenhouse, N. (2012). Changing climate, changing forests: The impacts of climate change on forests of the northeastern United States and eastern Canada. Gen. Tech. Rep. NRS-99. Newtown Square, PA: U.S. Department of Agriculture, Forest Service, Northern Research Station. 48 P. 99, 1–48.

Ryberg, K.R., and Vecchia, A.V., 2012, waterData—An R package for retrieval, analysis, and anomaly calculation of daily hydrologic time series data, version 1.0: *U.S. Geological Survey Open-File Report 2012–1168,* 8 p.

Seidl, R., Thom, D., Kautz, M., Martin-Benito, D., Peltoniemi, M., Vacchiano, G., Wild, J., Ascoli, D., Petr, M., Honkaniemi, J., *et al.* (2017). Forest disturbances under climate change. *Nature Climate Change 7,* 395–402.

Schweitzer, C., Clark, S.L., Gottschalk, K.W., Stringer, J., and Sitzlar, R. (2014). Proactive Restoration: Planning, Implementation, and Early Results of Silvicultural Strategies for Increasing Resilience against Gypsy Moth Infestation in Upland Oak Forests on the Daniel Boone National Forest, Kentucky. *Journal of Forestry; Bethesda 112*, 401–411.

Thornton, P.E., M.M. Thornton, B.W. Mayer, Y. Wei, R. Devarakonda, R.S. Vose, and R.B. Cook. 2018. Daymet: Daily Surface Weather Data on a 1-km Grid for North America, Version 3. ORNL DAAC, Oak Ridge, Tennessee, USA.

Thom, D., and Seidl, R. (2016). Natural disturbance impacts on ecosystem services and biodiversity in temperate and boreal forests. *Biological Reviews 91*, 760–781.

Turgenev, I.S. (1890). "*Zapiski ruzheinogo okhotnika Orenburgskoi gubernii* S. A--va. Moskva. 1852," *Polnoe sobranie sochinenii i pisem, Sochineniia*, vol. 4 (Moscow: Izdatel'stvo

Nauka, 1980), p. 516; translation quoted from Thomas P. Hodge, *Hunting Nature: Ivan Turgenev and the Organic World*, forthcoming

U.S. Geological Survey (USGS), U.S. Department of Agriculture - Natural Resource Conservation Service (NRCS), U.S. Environmental Protection Agency (EPA), and Other Federal, State, and local partners (see dataset specific metadata for details ftp://rockyftp.cr.usgs.gov/ngtoc/hydro/outgoing/WBDArchivedMetadata),20181205, USGS Watershed Boundary Dataset (WBD) for 2-digit Hydrologic Unit - 01 (published 20181205):

Weed, A.S., Ayres, M.P., and Hicke, J.A. (2013). Consequences of climate change for biotic disturbances in North American forests. *Ecological Monographs 83*, 441–470

Wehner, C.E., and Stednick, J.D. (2017). Effects of mountain pine beetle-killed forests on source water contributions to streamflow in headwater streams of the Colorado Rocky Mountains. Frontiers in *Earth Science 11*, 496–504.

APPENDIX

Supplemental Table 1: Mean Defoliation as a Function of Gage Drainage Size. Results of a linear model show the coefficient estimate and respective significance values for mean defoliation as a function of drainage size.

	Dependent Variable: Mean Watershed Defoliation		
Drainage (m^2) for different Gage Class	F-Value	Df	P-value
Reference Gage	1.049	(1,263)	0.307
All Gages	1.357	(1,34)	0.252

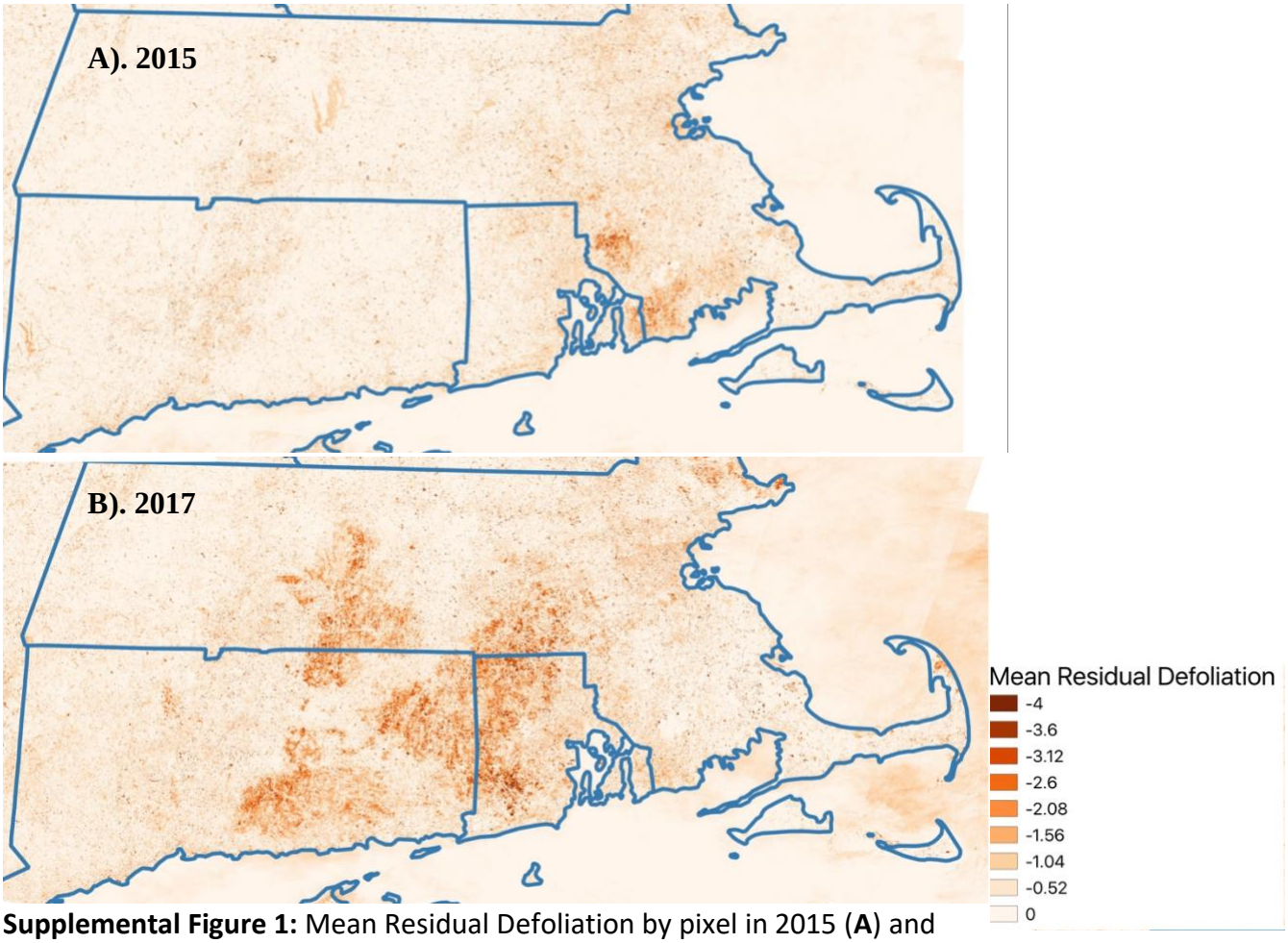

Supplemental Figure 1: Mean Residual Defoliation by pixel in 2015 (**A**) and 2017 (**B**) The scale of defoliation is the same in all years. (*Data sourced*: Pasquerella *et al.*, 2017).

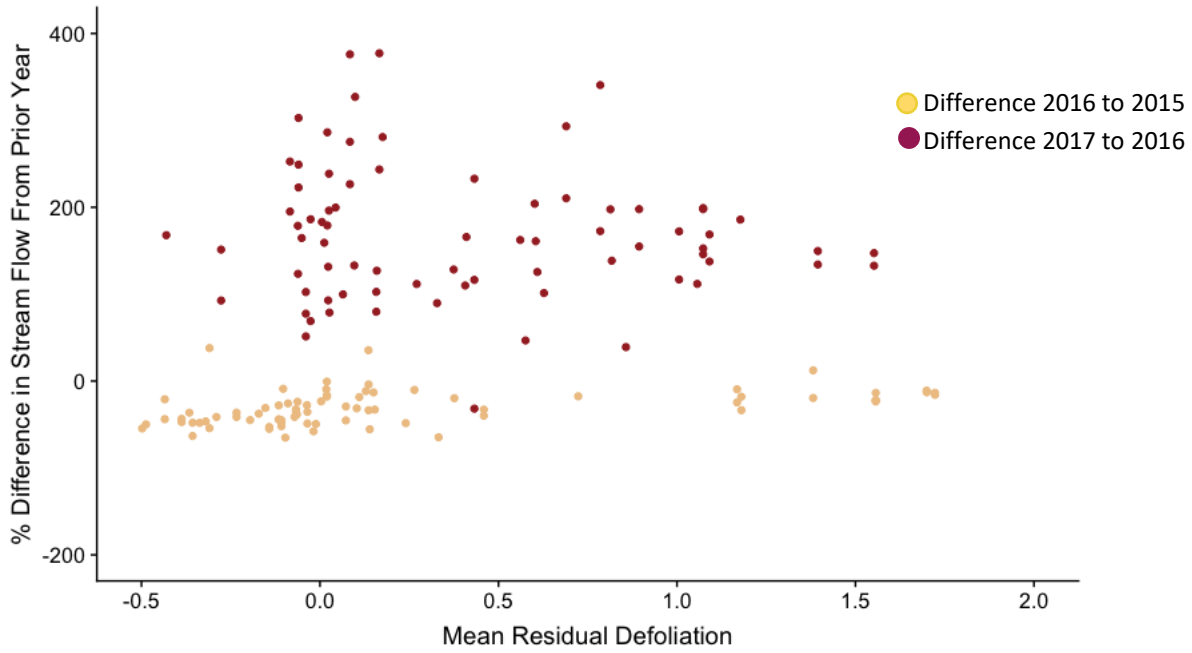

Supplemental Figure 2: % Difference in Stream Flow From Year Prior As a Function of Defoliation. Positive defoliation values correlate to higher values of defoliation 2015. Golden points compare difference of 2016 to 2015, red points compare difference of 2017 to 2016.

Supplemental Table 2: Stream gages used in study. Mean defoliation over the watershed extent is included for each stream gage for each year of the study.

Staid	Class	Drain (km^2)	Latitude	Longitude	State	Active years Since 1990	2015 Defol	2016 Defol	2017 Defol	Watershed Name
1127000	Non-ref	1838.699	41.60	-71.98	CT	19	0.39	-0.72	-1.18	Lower Quinebaug River
1119500	Non-ref	314.8461	41.75	-72.27	CT	20	0.49	0.15	-0.61	Willimantic River
1121000	Ref	70.25372	41.84	-72.17	CT	20	0.57	0.37	-0.60	Natchaug River
1127500	Non-ref	230.7345	41.56	-72.12	CT	20	0.29	-0.02	-0.56	Yantic River
1196620	Non-ref	63.81	41.42	-72.90	CT	20	0.48	-0.26	-0.33	Mill River-Frontal Long Island Sound
1199000	Non-ref	1643.036	41.96	-73.37	CT	19	0.72	0.36	-0.02	Konkapot River-Housatonic River
1199050	Non-ref	76.0986	41.94	-73.39	CT	19	0.72	0.36	-0.02	Konkapot River-Housatonic River
1195490	Non-ref	47.5542	41.60	-72.88	CT	20	0.29	-0.07	-0.16	Quinnipiac River
1196500	Non-ref	285.7488	41.45	-72.84	CT	20	0.29	-0.07	-0.16	Quinnipiac River
1195100	Ref	14.8383	41.31	-72.53	CT	20	0.25	-0.14	-0.63	Hammonasset River-Frontal Long Island Sound
1204000	Non-ref	195.2595	41.48	-73.22	CT	19	0.59	0.04	-0.10	Pomperaug River
1205500	Non-ref	3998.594	41.38	-73.17	CT	20	0.58	0.07	-0.06	Eightmile Brook-Housatonic River
1101500	Non-ref	115.2826	42.57	-71.03	MA	19	0.21	0.14	-0.01	Ipswich River
1102000	Non-ref	316.4265	42.66	-70.89	MA	20	0.21	0.14	-0.01	Ipswich River
1105600	Non-ref	12.6603	42.19	-70.94	MA	20	0.10	0.29	0.06	Hingham Bay
1103500	Non-ref	473.3199	42.26	-71.26	MA	20	0.33	0.12	0.06	Lower Charles River
1104200	Non-ref	548.3745	42.32	-71.23	MA	20	0.33	0.12	0.06	Lower Charles River
1104500	Non-ref	647.4123	42.37	-71.23	MA	20	0.33	0.12	0.06	Lower Charles River
1102500	Non-ref	59.74671	42.45	-71.14	MA	20	0.27	0.01	0.06	Mystic River
1208873	Non-ref	26.03027	41.18	-73.22	CT	19	0.33	-0.02	0.04	Pequonnock River-Frontal Long Island Sound
1208925	Non-ref	74.5146	41.17	-73.27	CT	19	0.33	-0.02	0.04	Pequonnock River-Frontal Long Island Sound
1208950	Ref	19.2393	41.15	-73.31	CT	19	0.33	-0.02	0.04	Pequonnock River-Frontal Long Island Sound
1101000	Non-ref	55.4778	42.75	-70.95	MA	20	0.04	-0.33	-0.67	Plum Island Sound
1122500	Non-ref	1048.47	41.70	-72.18	CT	20	0.43	-0.14	-0.89	Shetucket River
1123000	Ref	77.85271	41.67	-72.05	CT	20	0.43	-0.14	-0.89	Shetucket River
1097000	Non-ref	299.3094	42.43	-71.45	MA	20	0.39	0.11	-0.08	Concord River
1097300	Non-ref	30.8718	42.51	-71.40	MA	20	0.39	0.11	-0.08	Concord River
1099500	Non-ref	1035.51	42.64	-71.30	MA	20	0.39	0.11	-0.08	Concord River
1098530	Non-ref	274.2327	42.33	-71.40	MA	20	0.21	-0.14	-0.43	Sudbury River
1172500	Non-ref	142.6932	42.43	-72.02	MA	19	0.80	0.39	-0.17	Ware River
1173500	Non-ref	510.3333	42.24	-72.27	MA	20	0.80	0.39	-0.17	Ware River
1175670	Non-ref	23.9517	42.27	-72.00	MA	19	0.59	0.04	-0.69	Quaboag River
1176000	Non-ref	387.1593	42.18	-72.26	MA	19	0.59	0.04	-0.69	Quaboag River
1169900	Non-ref	62.30875	42.54	-72.69	MA	20	0.40	0.54	0.08	Lower Deerfield River
1170000	Non-ref	1451.378	42.54	-72.65	MA	19	0.40	0.54	0.08	Lower Deerfield River

Staid	Class	Drain (km^2)	Latitude	Longitude	State	Active years 1990	2015 Defol	2016 Defol	2017 Defol	Watershed Name
1174500	Non-ref	113.0355	42.39	-72.24	MA	20	0.34	0.31	-0.43	Swift River
1175500	Non-ref	489.9175	42.27	-72.33	MA	19	0.34	0.31	-0.43	Swift River
1181000	Ref	243.495	42.24	-72.90	MA	20	0.88	0.89	0.43	West Branch Westfield River
1177000	Non-ref	1785.374	42.16	-72.51	MA	20	0.33	0.06	-0.82	Chicopee River
1109070	Non-ref	27.1674	41.84	-71.14	MA	19	-0.08	0.10	0.63	Lower Taunton River
1105870	Non-ref	55.1439	41.99	-70.73	MA	19	0.18	0.43	0.82	North River-Frontal Massachusetts Bay
1105730	Non-ref	79.5672	42.10	-70.82	MA	20	0.18	0.43	0.82	North River-Frontal Massachusetts Bay
1105000	Non-ref	84.8778	42.18	-71.20	MA	20	0.13	0.07	-0.02	Neponset River
1105500	Non-ref	60.7122	42.15	-71.15	MA	20	0.13	0.07	-0.02	Neponset River
1110000	Non-ref	66.08279	42.23	-71.71	MA	20	0.57	0.02	-0.60	Upper Blackstone River
1184000	Non-ref	25049.46	41.99	-72.61	CT	20	0.35	0.10	-0.10	Mill River-Connecticut River
1184100	Non-ref	24.64571	41.96	-72.71	CT	20	0.35	0.10	-0.10	Mill River-Connecticut River
1111500	Non-ref	237.2391	42.00	-71.56	RI	20	0.03	-1.38	-1.39	Lower Blackstone River
1112500	Non-ref	1047.424	42.01	-71.50	RI	20	0.03	-1.38	-1.39	Lower Blackstone River
1109000	Non-ref	112.7429	41.95	-71.18	MA	20	-0.32	-0.46	-0.03	Threemile River
1109060	Non-ref	220.1049	41.87	-71.12	MA	20	-0.32	-0.46	-0.03	Threemile River
1197000	Non-ref	149.5539	42.47	-73.20	MA	20	0.68	0.71	0.28	Headwaters Housatonic River
1197500	Non-ref	732.8628	42.23	-73.35	MA	20	0.68	0.71	0.28	Headwaters Housatonic River
1109403	Non-ref	137.592	41.83	-71.35	RI	20	-0.13	-0.15	-0.41	Ten Mile River
1170500	Non-ref	20389.69	42.58	-72.57	MA	20	0.51	0.32	0.05	Manhan River-Connecticut River
1171500	Non-ref	139.7872	42.32	-72.67	MA	20	0.51	0.32	0.05	Manhan River-Connecticut River
1100600	Non-ref	96.4215	42.57	-71.21	MA	20	0.11	-0.24	-0.18	Shawsheen River
1094400	Non-ref	166.1607	42.58	-71.79	MA	20	1.09	0.67	0.62	North Nashua River
1094500	Non-ref	279.657	42.50	-71.72	MA	20	1.09	0.67	0.62	North Nashua River
1117350	Non-ref	25.2135	41.48	-71.55	RI	20	0.09	-1.56	-1.07	Upper Pawcatuck River
1117420	Non-ref	93.1356	41.48	-71.60	RI	20	0.09	-1.56	-1.07	Upper Pawcatuck River
1117468	Ref	25.3413	41.49	-71.63	RI	20	0.09	-1.56	-1.07	Upper Pawcatuck River
1117500	Non-ref	260.4375	41.45	-71.68	RI	20	0.09	-1.56	-1.07	Upper Pawcatuck River
1114500	Non-ref	98.8735	41.86	-71.49	RI	20	0.03	-1.17	-1.09	Moshassuck River-Woonasquatucket River
1114000	Non-ref	60.42774	41.83	-71.41	RI	19	0.03	-1.17	-1.09	Moshassuck River-Woonasquatucket River
1116000	Non-ref	168.2577	41.69	-71.57	RI	20	0.16	-1.70	-1.01	Pawtuxet River
1116500	Non-ref	525.0195	41.75	-71.45	RI	19	0.16	-1.70	-1.01	Pawtuxet River
1208500	Non-ref	674.4304	41.44	-73.06	CT	20	0.48	-0.10	-0.27	Outlet Naugatuck River
1117000	Non-ref	59.6844	41.64	-71.45	RI	20	-0.19	-0.38	-0.37	Narragansett Bay-Frontal Rhode Island Sound
1206900	Non-ref	260.7732	41.67	-73.07	CT	19	0.60	0.20	-0.16	Headwaters Naugatuck River
1183500	Non-ref	1292.801	42.11	-72.70	MA	20	0.58	0.34	-0.01	Outlet Westfield River

Staid	Class	Drain (km^2)	Latitude	Longitutde	State	Active years 1990	2015 Defol	2016 Defol	2017 Defol	Watershed Name
1185500	Non-ref	237.4254	42.08	-73.07	MA	20	0.78	0.61	0.03	West Branch Farmington River
1186000	Non-ref	333.5841	41.96	-73.02	CT	19	0.78	0.61	0.03	West Branch Farmington River
1208990	Ref	53.77249	41.29	-73.40	CT	20	0.39	0.09	-0.03	Saugatuck River-Frontal Long Island Sound
1187300	Ref	53.919	42.04	-72.94	MA	20	0.70	0.49	-0.04	East Branch Farmington River
1124000	Non-ref	392.0004	42.02	-71.96	CT	19	0.42	-0.15	-0.81	Upper Quinebaug River
1117800	Ref	90.76591	41.57	-71.72	RI	19	0.28	-1.72	-1.55	Wood River
1118000	Non-ref	193.2111	41.50	-71.72	RI	20	0.28	-1.72	-1.55	Wood River
1118300	Ref	10.3644	41.47	-71.83	CT	20	0.10	-1.18	-0.79	Lower Pawcatuck River
1118500	Non-ref	765.774	41.38	-71.83	RI	20	0.10	-1.18	-0.79	Lower Pawcatuck River
1192500	Non-ref	190.6678	41.78	-72.59	CT	19	0.21	0.00	-0.58	Hockanum River
1184490	Non-ref	38.06368	41.91	-72.55	CT	20	0.41	-0.11	-0.86	Scantic River
1193500	Ref	271.2563	41.55	-72.45	CT	19	0.40	0.06	-1.06	Salmon River
1192883	Non-ref	77.8588	41.52	-72.71	CT	20	0.22	-0.13	-0.41	Mattabesset River
1189995	Non-ref	1492.974	41.91	-72.76	CT	20	0.49	0.17	-0.14	Outlet Farmington River
1186500	Non-ref	221.4873	41.97	-73.03	CT	19	0.78	0.50	-0.01	Still River
1189000	Non-ref	116.4466	41.67	-72.90	CT	19	0.49	0.23	-0.27	Headwaters Farmington River
1188000	Ref	10.6235	41.79	-72.96	CT	19	0.49	0.23	-0.27	Headwaters Farmington River
1188090	Non-ref	977.783	41.76	-72.89	CT	19	0.49	0.23	-0.27	Headwaters Farmington River